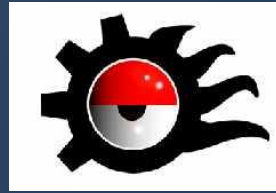


Instituto Politécnico Nacional

Centro de Investigación en Ciencia Aplicada y Tecnología Avanzada
CICATA, Legaria 694. Col. Irrigación, C.P. 11500, México D.F., México
<http://www.cicata.ipn.mx>



“BASIC PRINCIPLES OF PHOTOTHERMAL TECHNIQUES AND THEIR APPLICATIONS.”

by

ERNESTO MARÍN MOARES (Ph.D)

emarinm@ipn.mx emarin63@yahoo.es (preferable)



The Abdus Salam
International Centre
for Theoretical Physics

Winter College on Optics: Advanced Optical Techniques for Bio-Imaging
February 13-24, 2017



**RESEARCH CENTRE ON APPLIED SCIENCE AND
ADVANCED TECHNOLOGY (CICATA)
NATIONAL POLYTECHNICAL INSTITUTE (IPN), MEXICO CITY
<http://www.cicata.ipn.mx>**



**MASTER AND PHD PROGRAMS
IN ADVANCED TECHNOLOGY**

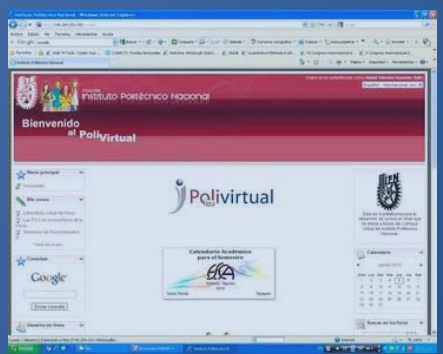
Research Areas

- 1- Nanotechnology and Functional Materials
- 2- Biomaterials.
- 2- Instrumentation and Characterization

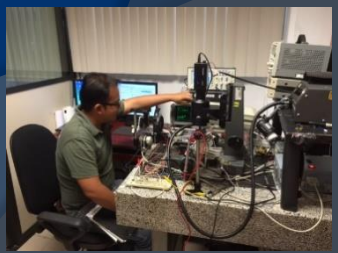
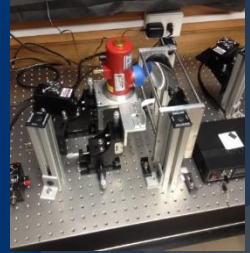
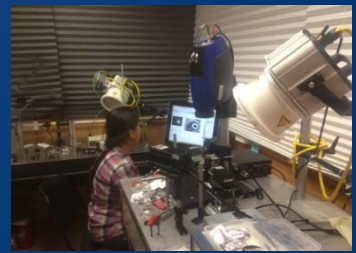
Since 2011 Graduate Programms of International Competence
PNPC-CONACyT
→ Scholarships (also for foreign students)

**MASTER AND PHD PROGRAMS
IN PHYSICS EDUCATION**

PHOTOTHERMAL TECHNIQUES LABORATORY



**MASTER AND PHD PROGRAMS
IN MATHEMATICS EDUCATION**



OUTLINE:

1. THE PHOTOACOUSTIC EFFECT

- WHY TO USE THE PA EFFECT FOR MATERIALS CHARACTERIZATION ?
- HEAT GENERATION AFTER LIGHT ABSORPTION:
- THE PHOTOACOUSTIC TECHNIQUE: EXPERIMENTAL SET-UP. WHAT IS MEASURED?

2. THERMAL WAVES PHYSICS

- OPTICAL ABSORPTION AND LIGHT INTO HEAT ENERGY CONVERSION
- THREE MODES OF HEAT TRANSFER
- 1 D HEAT CONDUCTION: THE HEAT DIFFUSION EQUATION
- THERMAL WAVES AND THEIR PROPERTIES

3. THE PHOTOTHERMAL TECHNIQUES

- BESIDES PHOTOACOUSTICS: HOW TO DETECT?
- SOME PHOTOTHERMAL TECHNIQUES

4. SELECTED APPLICATIONS :

- SPECTROSCOPY
- CALORIMETRY: THERMAL PROPERTIES MEASUREMENT
- DEPTH PROFILING
- IMAGING

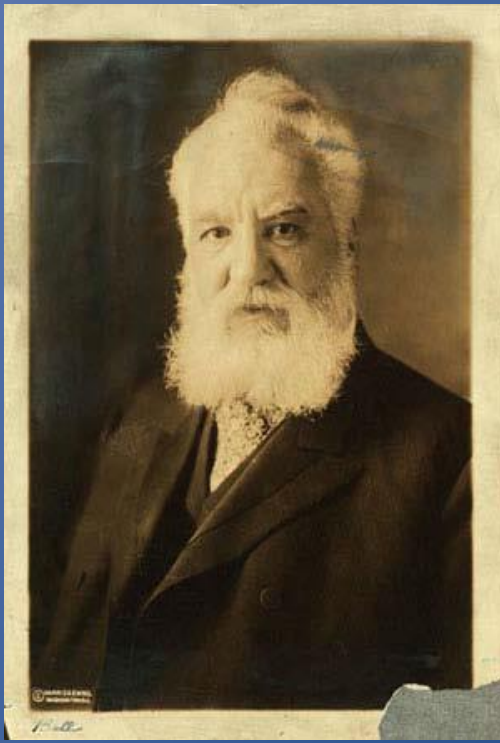
A LITTLE BIT OF HISTORY: REDISCOVERING 19 CENTURY DISCOVERIES BY MODERN SCIENCE

1ST PART: THE PHOTOACOUSTIC EFFECT

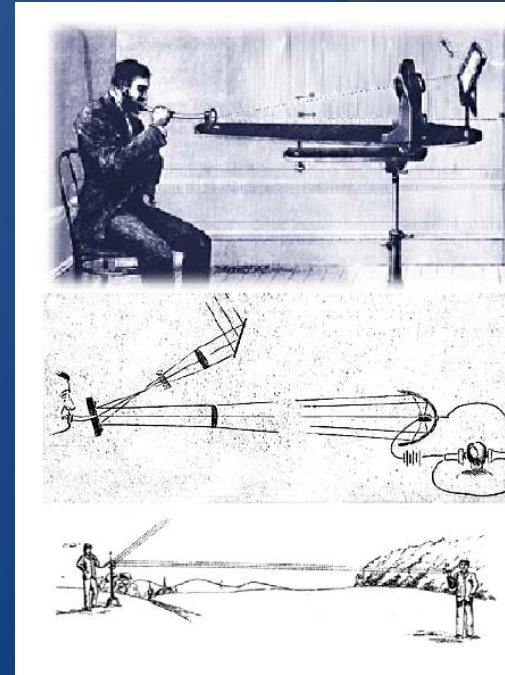
“HEARING LIGHT”

1880: the discovery

Bell, A. G., *Am. J. of Sci.* 20, 305 (1880).



Alexander Graham Bell (1847-1922)



Bell, A. G. y Tainter, S., *Photophone*
United State Patent No. 235, 496, (1880).

I have heard articulate speech produced by sunlight, I have heard a ray of the sun laugh and cough and sing! I have been able to heard a shadow, and I have even perceived by ear the passage of a cloud across the sun's disk...can imagination picture what the future of this invention is to be...

A. G. Bell. Fragment of 1880' Brief to Charles Sumner Tainter

facts were obtained from crystals of dichromate of potash, crystals of sulphate of copper, and from tobacco smoke. These experiments, which were made by Prof. Bell in Paris, were afterwards repeated and greatly extended in Washington by Mr. Talbot, with the modified apparatus shown in Fig. 1. In this, the materials experimented on were enclosed in a conical cavity of brass, closed by a flat plate of glass. A brass tube leading into the cavity served for connection with the hearing tube. With this apparatus Mr. Talbot examined the sonorous properties of a vast number of substances, and found that cotton wool, woolen, silk, and fibrous materials generally, produced much louder sounds than hard, rigid bodies like crystals, or diaphragms such as lead diaphragms have used. Furthermore, it was found that the darkest shades of alkali and waxed produced the best effects. This observation suggested the trial of lampblack. A piece of smoked glass held in the set-screw beam of sunlight, with the lampblack surface towards the sun, produced a

of articulation under the action of an undulatory beam from the transmitter used with the photophone, (see page 22 of our January number for this year).



The general conditions arrived at from a great number of experiments with solid substances, are that the loudest sounds are produced from substances in a loose, porous, spongy condition, and from those that have the darkest or most absorbent colors. The materials giving the best effects are cotton wool, woolen, fibrous materials generally, such as sponge, platinum and other metals in a spongy condition, and lampblack.

Prof. Bell explains the loud, sonorous effects produced from such substances as follows: Taking the case of lampblack as an example, a substance which becomes heated by rays of all refrangibility, he considers a mass of this substance as a spongy mass, with its pores filled with air instead of water. When a

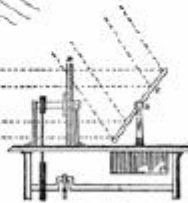


Fig. 3.

sound loud enough to be heard with attention in any part of the room.

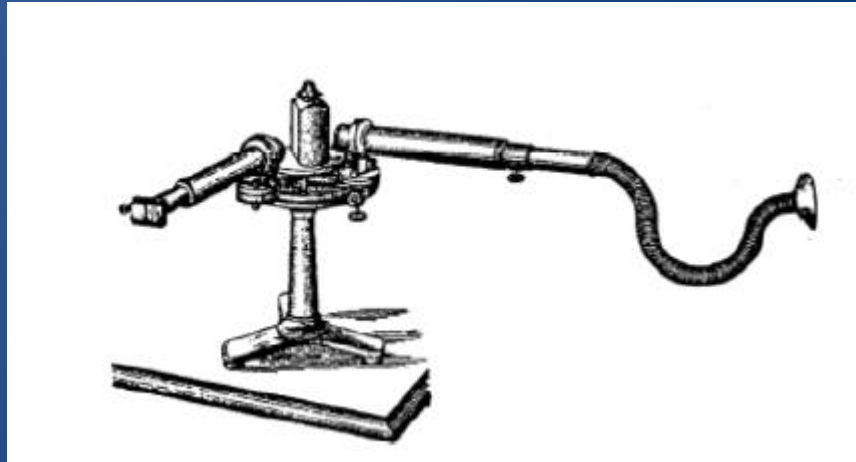
These experiments were repeated and verified by Mr. Bell on his return from Paris. By smoking the interior of the conical cavity of Fig. 1, and exposing it

The experiments made to verify this suggestion succeeded with lampblack.

Fig. 1 illustrates the mode in which the experiment was conducted. A represents the diaphragm of the transmitter, and B the lampblack receiver with hear-

beam of sunlight falls upon this mass, the particles of lampblack are heated, and consequently expand, causing a contraction of the air spaces among them. Under such circumstances a pulse of air should be expelled, as water is expelled by sudden pressure upon a

BELL'S EXPERIMENTAL SET-UP TO STUDY THE PHOTOACOUSTIC EFFECT



SPECTROPHONE

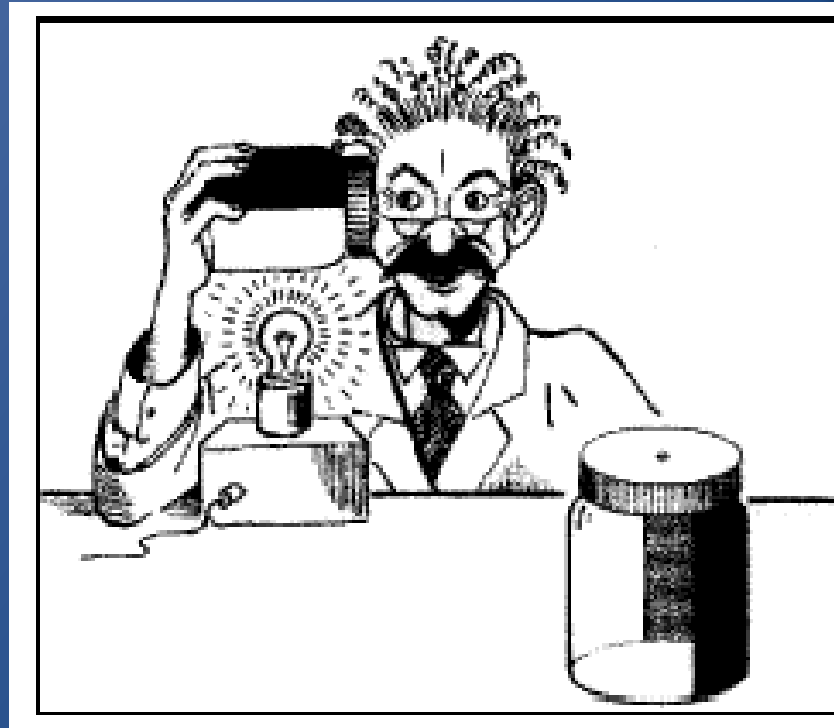
The Manufacturer and Builder Volume 0013 Issue 7 p. 156 (July 1881)



**HOME WORK:
DEMONSTRATING THE PHOTOACOUSTIC EFFECT WITH A STETHOSCOPE**

Lat. Am. J. Phys. Educ. Vol. 2, No. 2, May 2008

OTHER “KITCHEN” EXPERIMENTS



Rush, W. F. and Heubler, E. 1982 *Am. J. Phys.* **50** 669.

Campbell, C. and Laherrere 1998 *J. Sci. Am.* **78** 278.

Euler, M., Niemann, K. and Müller, A. 2000 *Phys. Teacher* **38** 356

Euler, M., *Phys. Teacher* 2001 **39** 406.

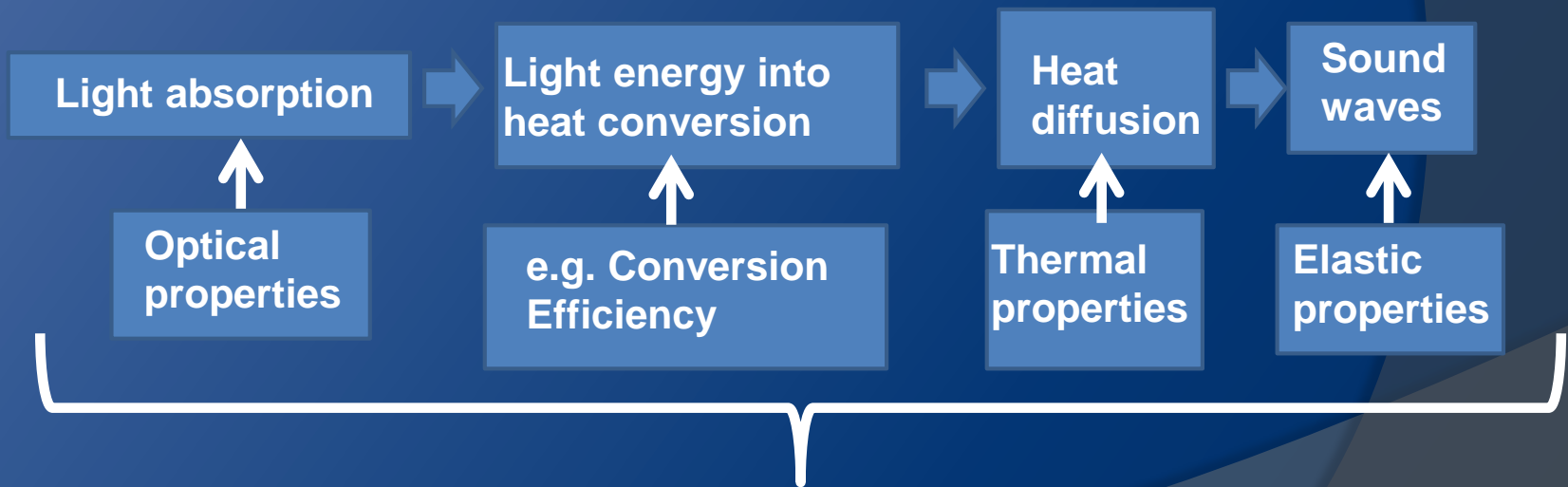
Modulated light beam



INTERPRETATION OF HOMEWORK RESULTS



Mechanisms involved in the generation of the photoacoustic signal



MOTIVATION:
WHY TO USE SUCH EFFECT FOR MATERIALS CHARACTERIZATION

RAW ESTIMATION: ORDERS OF MAGNITUDE

Power: 0.1 mW

Duration: 5.0 ms

→ $Q = 5.0 \times 10^{-7} \text{ J}$

Light pulse

$\Delta T = ?$

$$Q = m c \Delta T$$

$$c_{\text{air}} = 1.0 \text{ J/gK}$$

$$\rightarrow \Delta T = 4.2 \times 10^{-4} \text{ K}$$

$\Delta P = ?$

Before de light pulse

$$P_0 V = n R T_0$$

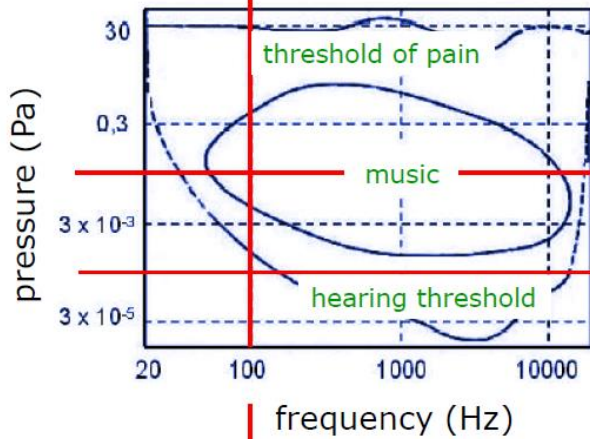
After de pulse

$$(P_0 + \Delta P) V = n R (T_0 + \Delta T)$$

$$\rightarrow \Delta P = P_0 (\Delta T / T_0)$$

$$\rightarrow \Delta P = 4.0 \times 10^{-2} \text{ Pa}$$

1.0 cm³ of air



$4,0 \times 10^{-2} \text{ Pa}$

$\Delta T = 10^{-6} \text{ K}$
 $3,3 \times 10^{-4} \text{ Pa}$



A. M. Mansanares, Short Course at V International Conference on Surfaces, Materials and Vacuum
 September 24 -28, 2012 Tuxtla Gutiérrez, Chiapas, Mexico

MOTIVATION:

HOW TO DETECT SO SMALL VARIATIONS IN PRESSURE (OR TEMPERATURE) ?

EARLY WORKS

Bell A G 1881 *Nature* **24** 42

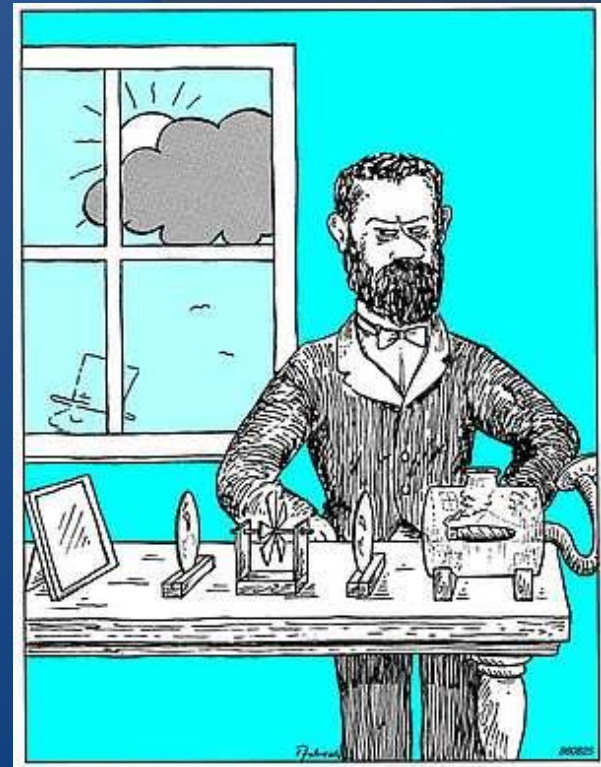
Tyndall J 1881 *Proc. R. Soc. Lond.* **31** 307

Roentgen W 1881 *Phil. Mag.* **11** 308

-
-
-

Viengerov, M. L. 1938 *Dokl. Akad. Nauk. SSSR* **19** 687

Luft K F 1954 *C. R. Hebd. Seances Acad. Sci.* **238** 1651



Theory of the photoacoustic effect with solids

Allan Rosenzweig and Allen Gersho

Bell Laboratories, Murray Hill, New Jersey 07974
(Received 24 July 1975)

When chopped light impinges on a solid in an enclosed cell, an acoustic signal is produced within the cell. This effect is the basis of a new spectroscopic technique for the study of solid and semisolid matter. A quantitative derivation is presented for the acoustic signal in terms of the optical, thermal, and geometric parameters of the system. The theory predicts the dependence of the signal on the absorption coefficient of the solid, thereby giving a theoretical foundation for the technique of photoacoustic spectroscopy. In particular, the theory accounts for the experimental observations that with this technique optical absorption spectra can be obtained for materials that are optically opaque.

PACS numbers: 78.20.H, 43.35., 07.45.

I. INTRODUCTION

In 1880, Alexander Graham Bell¹ discovered that when a periodically interrupted beam of sunlight shines on a solid in an enclosed cell, an audible sound could be heard by means of a hearing tube attached to the cell. Motivated by Bell's discovery, Tyndall² and Röntgen³ found that an acoustic signal can also be produced when a gas in an enclosed cell is illuminated with chopped light. Bell subsequently experimented with a variety of solids, liquids, and gases and his work generated a brief flurry of interest. The photoacoustic effect was evidently regarded as a curiosity of no practical value and was soon forgotten. Fifty years later the photoacoustic or photoacoustic effect with gases was reexamined. It has since become a well-established technique for gas analysis and is well understood. Photons absorbed by the gas are converted into kinetic energy of the gas molecules, thereby giving rise to pressure fluctuations within the cell. The photoacoustic effect with solids, however, was apparently ignored for 80 years and a satisfactory theoretical explanation of the effect with solids was never published.

Recently, interest in the photoacoustic effect with solids has been revived with the development of a very useful technique for spectroscopic investigation of solid and semisolid materials.⁴⁻⁶ The name change from optoacoustic to photoacoustic has been instituted to reduce confusion with the acousto-optic effect in which a laser beam is deflected by acoustic waves in a crystal.

In photoacoustic spectroscopy of solids, or PAS, the sample to be studied is placed inside a closed cell containing a gas, such as air, and a sensitive microphone. The sample is then illuminated with chopped monochromatic light. The analog signal from the microphone is applied to a tuned amplifier whose output is recorded as a function of the wavelength of the incident light. In this way photoacoustic spectra are obtained and these spectra have been found to correspond, qualitatively at least, to the optical absorption spectra of the solids.

One of the principal advantages of photoacoustic spectroscopy is that it enables one to obtain spectra similar to optical absorption spectra on any type of solid or semisolid material, whether it be crystalline, powder, amorphous, smear, gel, etc. This capability is based on the fact that only the absorbed light is converted to sound. Scattered light, which presents such a

serious problem when dealing with many solid materials by conventional spectroscopic techniques, presents no difficulties in photoacoustic spectroscopy. Furthermore, it has been found experimentally that good optical absorption data can be obtained, with the photoacoustic technique, on materials that are completely opaque to transmitted light.⁴ Photoacoustic spectroscopy has already found some important applications in research and analysis of inorganic, organic, and biological solids and semisolids.⁴⁻⁶ It furthermore has very strong potential as a spectroscopic technique not only in the study of bulk optical properties, but also in surface studies and desiccation studies.⁷ With the rapid growth of interest in PAS, a quantitative understanding of the production of the acoustic signal is of utmost importance. In this paper we lay the groundwork for this analysis. In addition we have, for the first time, been able to account for the capability of the photoacoustic technique to derive optical absorption spectra from systems that are completely opaque to transmitted light.

Bell¹ attributed the photoacoustic effect observed with spongy solids such as carbon black to a cyclic driving off of pulses of air from, and reabsorption onto, the pores of the solid in response to the cyclical heating and cooling of the solid by the chopped light. He also supported the theory of Rayleigh⁸ who concluded that the effect is also probably due to a mechanical motion of the solid. However, Preece¹¹ inferred from his experiments that the solid does not undergo any substantial mechanical motion, and suggested that the effect was due to an expansion and contraction of the air in the cell. Mercadier¹² who also experimented with the effect concluded that the sound is due to "vibratory movement determined by the alternate heating and cooling produced by the intermittent radiations, principally in the gaseous layer adhering to the solid surface hit by these radiations."

We have found, from experiments in which we first thoroughly evacuated the photoacoustic cell and then refilled it with nonadsorbing noble gases and then experiments with two-dimensional solids and other materials with weak surface adsorption properties, that adsorbed gases do not play a significant role in the production of the acoustic signal. Furthermore, it can be readily shown that thermal expansion and contraction of the solid, and any thermally induced mechanical vibration of the solid are generally too small in magnitude to account for the observed acoustic signal. From

Photoacoustic spectroscopy of solids

The generation of sound from a periodically illuminated solid, an effect first discovered in 1881, is now being used to study the properties of materials not accessible to optical spectroscopy.

Allan Rosenzweig

One of the most effective means for studying the properties of matter non-destructively is to observe how photons interact with it; that is, by optical spectroscopy. The two most common techniques in the optical region are absorption and reflection spectroscopy. But many organic and inorganic materials, such as powders, amorphous compounds, smears, gels and oils, can not be readily studied by either of these two techniques. Methods involving diffuse or attenuated total reflectance permit the study of some of these materials, but they possess severe drawbacks.

A new technique recently developed at Bell Laboratories for the investigation of solid and semisolid matter⁴ overcomes many of these drawbacks. In this new technique, called "photoacoustic spectroscopy," modulated light absorbed by a sample is converted into sound, which is then detected by a microphone. Its principal advantage is that it permits us to obtain spectra similar to those from optical-absorption spectroscopy on any type of solid or semisolid material. Scattered light, which presents such a severe problem when we deal with many solid and semisolid materials by conventional techniques, presents no difficulties in photoacoustic spectroscopy because only the absorbed light is converted into sound. I have found that photoacoustic spectroscopy can be a very useful tool for research and analysis, not only in physics and chemistry but also in biology and medicine.⁴⁻⁶ Before examining these applications, let us briefly look at

Allan Rosenzweig is a member of the technical staff of Bell Laboratories, Murray Hill, N.J.

the history of photoacoustic spectroscopy and its theory.

What causes the effect?

Photoacoustic spectroscopy has its historical roots in the 1880's when Alexander Graham Bell, John Tyndall and Wilhelm Röntgen first studied¹ the so-called "opto-acoustic effect." This effect occurs when a gas in an enclosed cell is illuminated with periodically interrupted light. Energy absorbed by the gas is converted into kinetic energy of the gas molecules, giving rise to pressure fluctuations within the cell. These pressure fluctuations were detected in 1881 as audible sound through a hearing tube.

The opto-acoustic effect, here called the photoacoustic effect (to remove confusion with the "acousto-optic effect," wherein a laser beam interacts with acoustic waves in a crystal) has been used fairly extensively since then, primarily for gas analysis. More recently it was used by Lloyd Kreuzer and Kumar Patel² to study gaseous pollutants and by Mel Robin and his co-workers³ to perform studies on photochemical and kinetic effects in gases. Although the photoacoustic technique has been thoroughly developed for gases, the analogous effects in solids and liquids were apparently not studied until recently, despite initial experiments along these lines by Bell in 1881.

In photoacoustic spectroscopy of solids, the sample is placed inside a specially designed closed cell containing air (or other suitable gas) and a sensitive microphone. The solid is then illuminated with chopped monochromatic light, as figure 1 indicates.

Bell had attributed the presence of an acoustic signal from a solid to a cyclic process in which gases are driven off, and reabsorbed onto, the surface in response to the cyclical heating and cooling effect of the chopped light. However, I have found, from experiments in which I thoroughly evacuated the photoacoustic cell and then refilled it with nonadsorbing noble gases as well as from experiments with two-dimensional solids and other systems with weak surface-adsorption properties, that adsorbed gases generally do not play a significant role in the production of the acoustic signal. I have also shown that the cyclical expansion and contraction of the solid cannot be the major source of the signal. I have therefore concluded from these experiments along with the theory outlined below that the primary source of the acoustic signal arises instead from the periodic heat flow from the solid to the surrounding gas, as the solid is cyclically heated by the absorption of the chopped light. This conclusion was independently arrived at by John Parker at Johns Hopkins University.

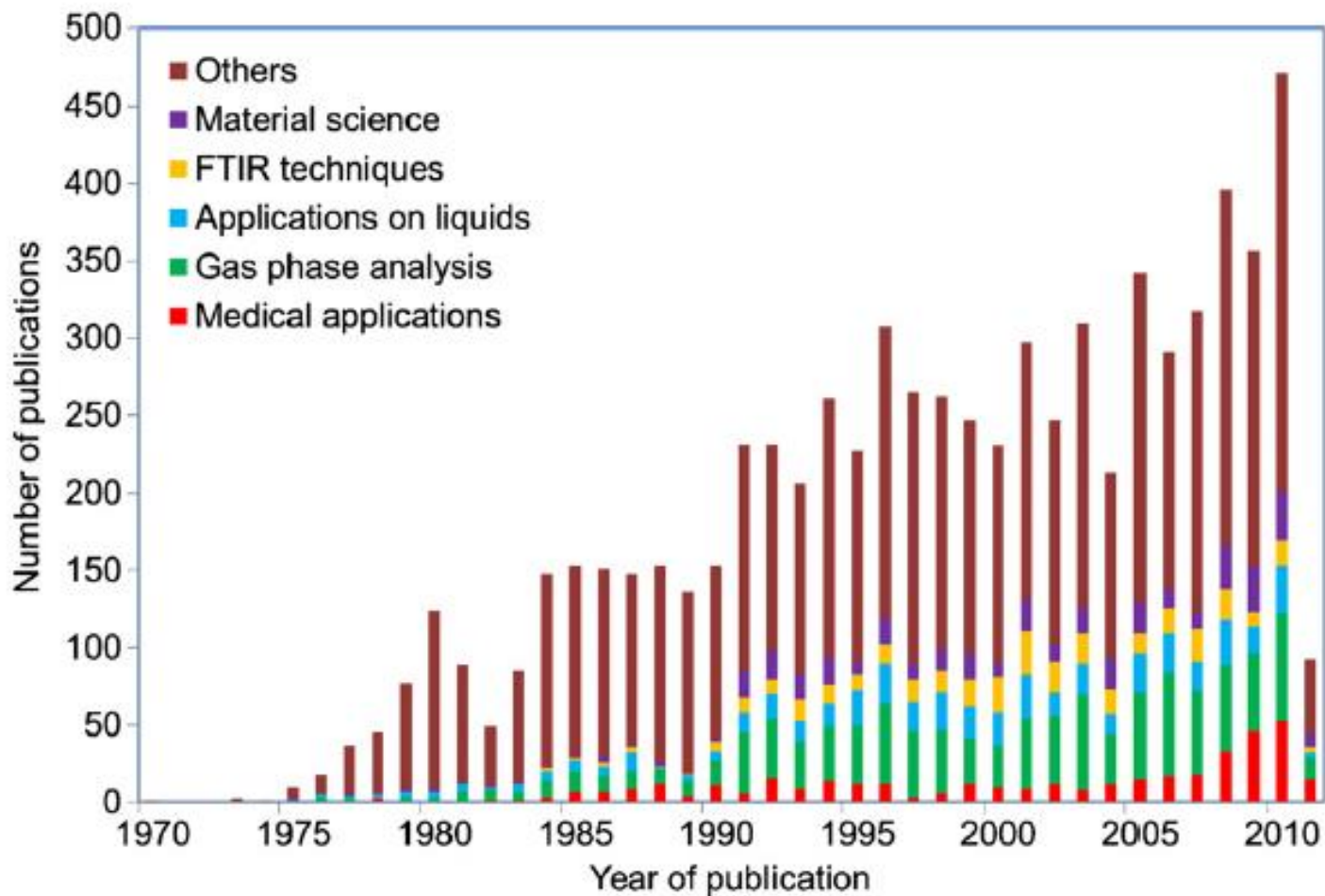
Nonradiative de-excitation processes convert part or all of the light absorbed by the solid into heat. The periodic flow of this heat into the gas of the cell produces pressure fluctuations in it; this is how the sound originates. In an experiment, these fluctuations are then detected by the microphone. The analog signal from the microphone is recorded as a function of the wavelength of the incident light. Suitable normalization procedures remove the spectral structures of the light source, the monochromator and so on.

PHYSICS TODAY / SEPTEMBER 1975 23

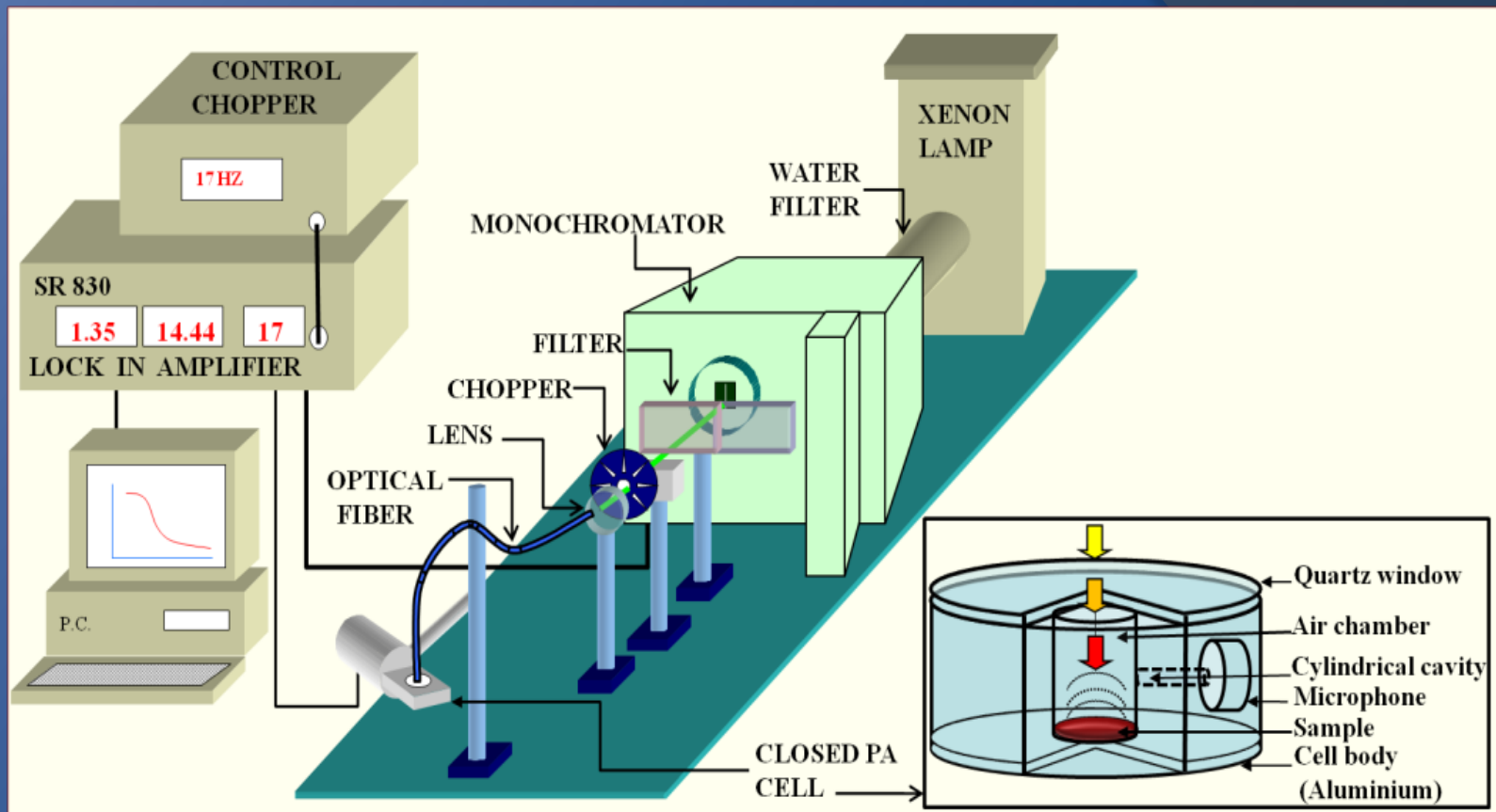
PHOTOACOUSTIC SPECTROSCOPY

→ First theoretical model

→ First applications



Number of publications on different fields of PA applications according to the ISI web of science statistics.



Schema of a typical experimental set-up

F. Gordillo Delgado, 2011 "Photoacoustic technique applied to the strengthening of clean agriculture"
Ph. D. Thesis, CICATA-Legaria México D.F.

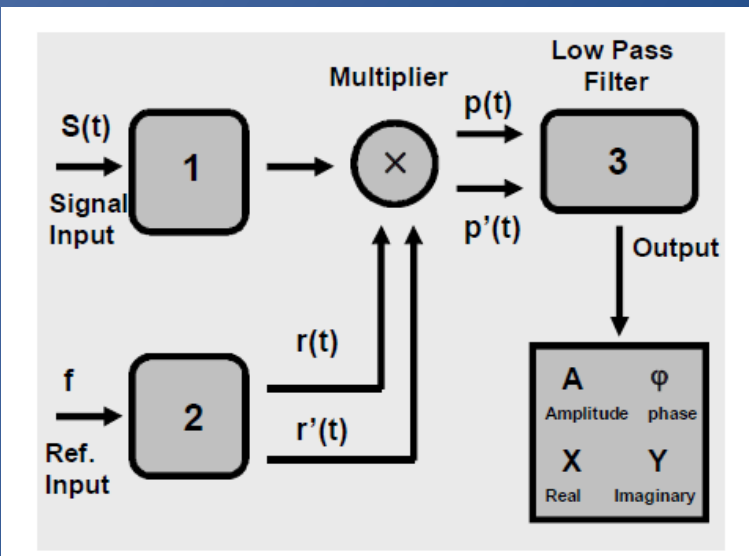
Small $\Delta T \rightarrow$ Small Signal to Noise Ratio \rightarrow Phase sensitive detection: The Lock-in Amplifier (LIA)

LIA in a Nut Shell

Lat. Am. J. Phys. Educ. Vol.3, No. 3, Sept. 2009

$S = A \cos(\omega t + \phi) + n$
signal to be measured

A: signal amplitude;
 ϕ : signal phase
 $\omega = 2\pi f$: angular frequency
n: noise at f



$r = 2 \cos(\omega t)$
 $r' = 2 \sin(\omega t)$

$p = S \times r = A \cos(\phi) + A \cos(2\omega t + \phi) + 2n \cos(\omega t)$

$p' = S \times r' = A \sin(\phi) + A \sin(2\omega t + \phi) + 2n \sin(\omega t)$

X and Y real (in-phase) and imaginary (quadrature) parts of the complex number $A \exp(i\phi)$; $i = (-1)^{1/2}$

$A = (X^2 + Y^2)^{1/2}$
 $\phi = \text{atan}(Y/X)$

$X = A \cos(\phi)$
 $Y = A \sin(\phi)$



SR810 LIA from Stanford Research Systems
~ \$ 4000



CICATA-FPGA LIA
Field Programmable Gate Array FPGA Spartan-3E
~ \$ 400

Measurement 69 (2015) 31-41

Wavelength (λ)-resolved experiments (PA-spectroscopy)(f -fixed)

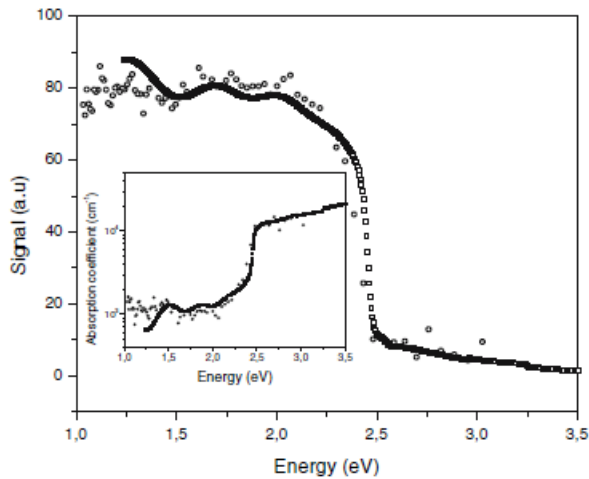


Fig. 1 A comparison between the optical properties obtained from PAS (circles) and conventional optical transmission (squares) measurements for a CdS sample (2 μm of thickness) grown by CSVT on glass substrates. The light modulation frequency used for PAS was 17 Hz

J Mater Sci (2007) 42:7176–7179

Modulation frequency (f)-resolved (λ fixed) Determination of transport parameters

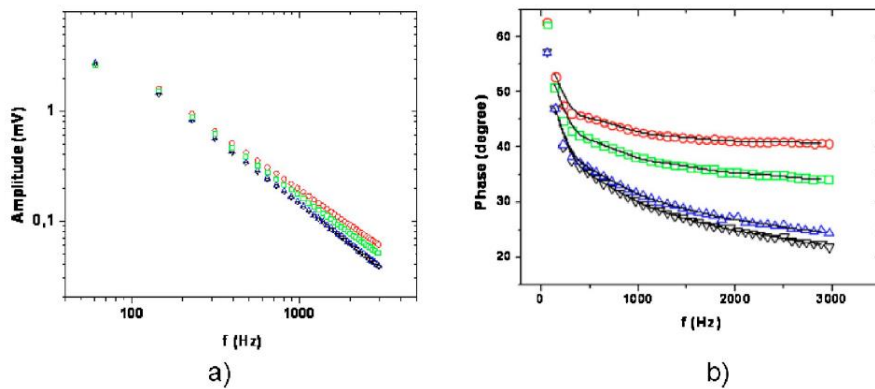


FIG. 4. (Color online) The amplitude (a) and the phase (b) of the PA signal as the function of the modulation frequency. Circles: correspond to samples where the CdS layers were grown by CSVT and the CdTe film by CSVT. Squares: S/Cd=2.5. Up-triangles: S/Cd=6. Down-triangles: S/Cd=5. The solid line is the result of the best fit using the theoretical model.

J. Appl. Phys. 107, 123701 (2010)

Time-resolved (both f and λ fixed) Monitoring of dynamic processes

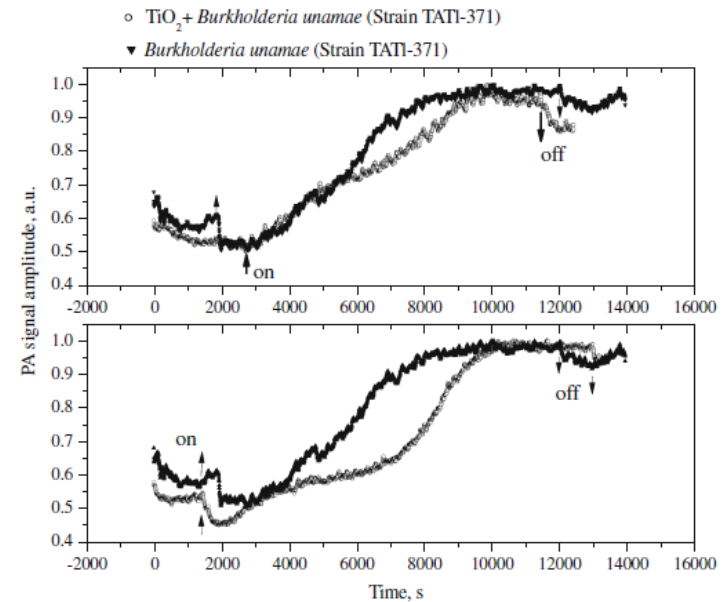


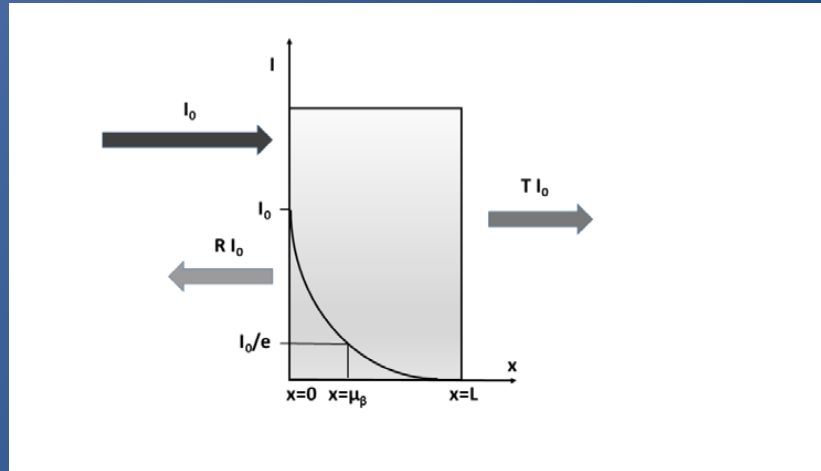
Fig. 2 PA signal amplitude as a function of time. Triangles correspond to the PA response of *B. unamae* (Strain TATI-371) and the circles curve corresponds to the PA response including the photobaric effect due to the photocatalytic activity of TiO₂ film on this same bacteria. The up and down arrows indicate the time instants at which a non-modulated white light Xe lamp, used to induce the photocatalytic process, is turned on and off, respectively. Both curves correspond to scans of two samples of the same culture

Int J Thermophys
DOI 10.1007/s10765-012-1330-x

2ND PART: THERMAL WAVE PHYSICS

OPTICAL ABSORPTION

Lambert-Beer law



Light Intensity [Wm^{-2}]

$$I = I_0 \exp(-\beta x) = I_0 \exp(-x/\mu\beta)$$

Absorbance

Molar Concentration [M]

$I(x=0)$ Optical absorption coefficient

Light penetration depth = $1/\beta$

$$A = \chi L C_m \quad *$$

$$A = -\ln(T) = \ln(I_0/I) = \beta L \quad **$$

Molar Absorptivity Coefficient [$\text{M}^{-1}\text{m}^{-1}$]
(λ -dependent)

$$T = I/I_0 \quad \text{Transmittance}$$

Reflectance

$$* \quad + \quad * \quad * \quad \rightarrow \quad \beta = \chi C_m$$

$$A = R + T$$

LIGHT INTO HEAT ENERGY CONVERSION

amount of heat generated per volume unit of the sample in an element of thickness dx at depth x

$$dQ = -\eta(1-R)(dI/dx)dx + I = I_0 \exp(-\beta x) \rightarrow dQ = \eta(1-R)I_0\beta \exp(-\beta x)dx$$

quantum efficiency for heating
= produced heat / incident energy

THREE MODES OF HEAT TRANSFER

1- Convection

Heat flux density [W/m²]

$$\Phi_{\text{conv}} = q_{\text{conv}}/A = h_{\text{conv}}\Delta T$$

Newton's law

Convection heat transfer coefficient

2- Radiation

$$\Phi_{\text{rad}} = q_{\text{rad}}/A = \sigma e (T_0^4 - T^4)$$

Stefan-Boltzmann law

$T - T_0 \ll T_0 \rightarrow$

$$\Phi_{\text{rad}} = 4\sigma e T_0^3 (T - T_0) = h_{\text{rad}}\Delta T$$

3- Conduction

$$\Phi_{\text{cond}} = q_{\text{cond}}/A = -k\nabla T$$

Fourier's law

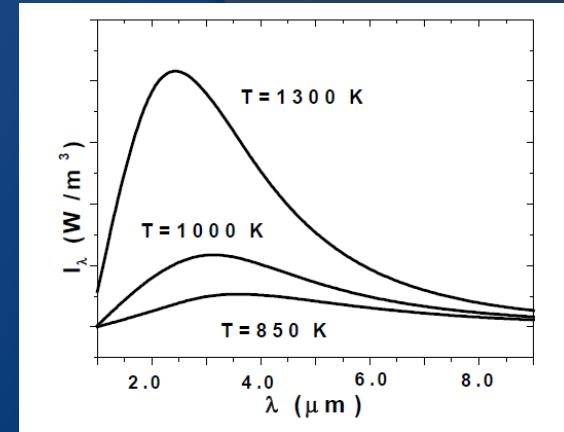
Radiation heat transfer coefficient

$$h_{\text{rad}} = 4\sigma e T_0^3$$

Conduction heat transfer coefficient

$$h_{\text{cond}} = k/L$$

The spectral intensity as a function of wavelength for a black body



1D, homogeneous and isotropic samples, $\rightarrow \nabla T$ small

$$\Phi_{cond} = k \frac{T_2 - T_1}{x_2 - x_1} = \frac{KA\Delta T}{L} = h_{cond}\Delta T \quad \rightarrow \quad q_{cond} = \frac{KA\Delta T}{L} = \frac{\Delta T}{R_{cond}}$$

Ohm's law for thermal conduction

$$R_{cond} = \frac{L}{Ak} = \frac{1}{Ah_{cond}} \quad \text{Thermal resistance (against conduction)}$$

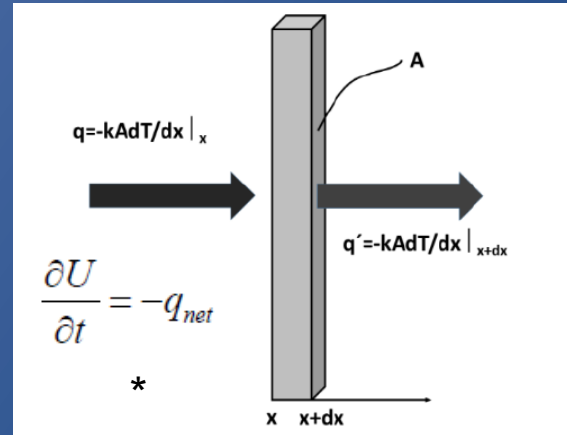
$$H = h_{conv} + h_{cond} = 1/(AR)$$

R: resistance (against convection-radiation)

$$B_i = \frac{H}{h_{cond}} = \frac{R_{cond}}{R}$$

Biot's number : fraction of material's thermal resistance that opposes to convection-radiation heat losses

FOURIER'S LAW + ENERGY CONSERVATION LAW → HEAT DIFFUSION EQUATION



$$(dx = \delta x, \text{ where } \delta x \rightarrow 0)$$

$$m = \rho \delta V = \rho A \delta x$$

First law of thermodynamics

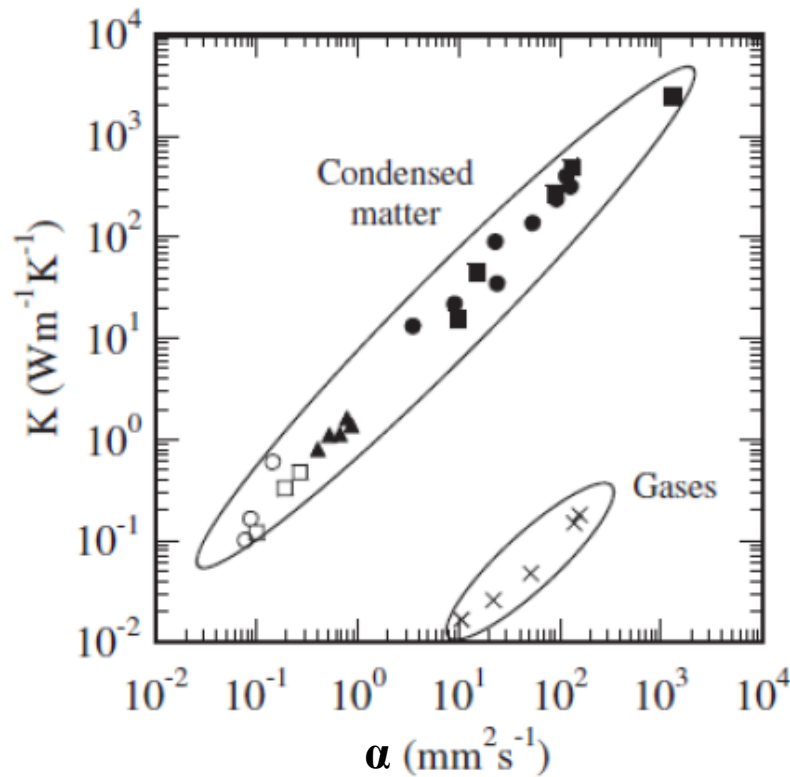
$$q_{net} = -kA \left\{ \frac{\partial T}{\partial x} \Big|_{x+\delta x} - \frac{\partial T}{\partial x} \Big|_{x+\delta x} \right\} = -kA \left\{ \frac{\frac{\partial T}{\partial x} \Big|_{x+\delta x} - \frac{\partial T}{\partial x} \Big|_{x+\delta x}}{\delta x} \right\} \delta x = -kA \frac{\partial^2 T}{\partial x^2} \delta x \quad **$$

$$\frac{\partial U}{\partial t} = mc \frac{\partial T}{\partial t} \quad ***$$

* + ** + *** → $\nabla^2 T - \frac{1}{\alpha} \frac{\partial T}{\partial t} = 0$ Heat diffusion equation

$$\alpha = k / \rho c$$

Thermal diffusivity



$$\alpha = k / \rho c$$



$$k = C \alpha$$

$$C = \rho c$$

Thermal conductivity versus thermal diffusivity

Closed circles: metals; squares: ceramics; triangles: glasses; open squares: polymers; open circles: liquids; crosses: gases

$$\text{Slope} \sim \rho c = k / \alpha \sim 3 \times 10^6 \text{ Jm}^{-3} \text{ K}^{-1}$$

THERMAL WAVES AND THEIR PROPERTIES

[Almond and Patel, 1996] Almond, D. P. and Patel, P. M. 1996, "Photothermal Science and Techniques" in "Physics and its Applications, 10", E.R. Dobbsand and S.B. Palmer (Eds), Chapman and Hall, London.

Isotropic and homogeneous semi-infinite solid + Superficial uniform light absorption (1D) + $\eta = 1$ + $R=0$ + neglecting heat losses (with H)

International Journal of Thermal Sciences 98 (2015) 202–207

$$\frac{\partial^2 T(x,t)}{\partial x^2} - \frac{1}{\alpha} \frac{\partial T(x,t)}{\partial t} = 0, \quad x > 0, \quad t > 0$$

HDE

$$-k \left. \frac{\partial T(x,t)}{\partial x} \right|_{x=0} = \frac{I_0}{2} \operatorname{Re}[(1 + \exp(i\omega t))]$$

BC

$$\frac{\partial^2 \theta(x,t)}{\partial x^2} - q^2 \theta(x) = 0$$

$$T(x,t) = \theta(x) \exp(i\omega t) \rightarrow$$

$$q = \sqrt{\frac{i\omega}{\alpha}} = \frac{(1+i)}{\mu}$$

$$\mu = \sqrt{\frac{2\alpha}{\omega}}$$

$$-k \left. \frac{\partial \theta(x,t)}{\partial x} \right|_{x=0} = \operatorname{Re} \left[\frac{I_0}{2} \exp(i\omega t) \right]$$

Wave number Thermal diffusion length

$$T(x,t) = \frac{I_0}{2\varepsilon\sqrt{\omega}} \exp(-qx) \exp\left[-i\left(\omega t + \frac{\pi}{4}\right)\right] = \frac{I_0}{2\varepsilon\sqrt{\omega}} \exp\left(-\frac{x}{\mu}\right) \exp\left[-i\left(\frac{x}{\mu} + \omega t + \frac{\pi}{4}\right)\right]$$

THERMAL WAVE EQUATION

Thermal properties determination is possible !

$$\varepsilon = k/\alpha^{1/2} = (Ck)^{1/2}$$

$$C = \rho c$$

Thermal effusivity $\sim k$ because the almost constancy of C

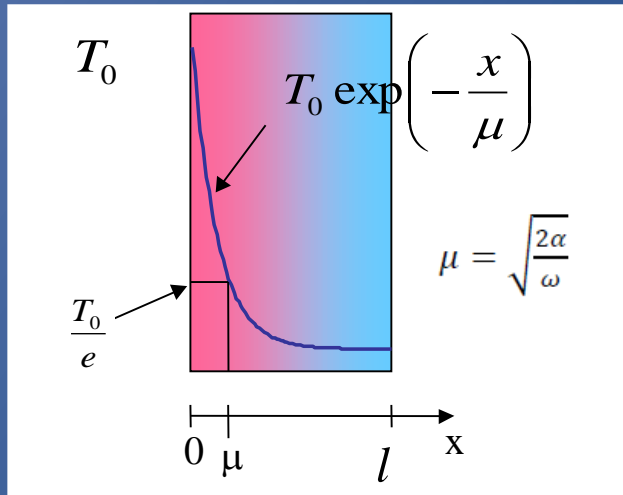
THERMAL WAVES AND THEIR PROPERTIES

$$T(x, t) = \frac{I_0}{2\varepsilon\sqrt{\omega}} \exp(-qx) \exp\left[-i\left(\omega t + \frac{\pi}{4}\right)\right] = \frac{I_0}{2\varepsilon\sqrt{\omega}} \exp\left(-\frac{x}{\mu}\right) \exp\left[-i\left(\frac{x}{\mu} + \omega t + \frac{\pi}{4}\right)\right]$$

Amplitude

Phase

$$\Delta\phi = x/\mu + \pi/4$$



Thermal diffusion length

$$Z_t = \frac{T(x=0, t) - T_{amb}}{-k \frac{dT(x, t)}{dx} \Big|_{x=0}}$$

$$Z_t = \frac{1-i}{\varepsilon\sqrt{\omega}} = \frac{1}{\varepsilon\sqrt{\omega}} \exp\left(-i\frac{\pi}{4}\right)$$

Thermal impedance

$$T(x, t) = \frac{I_0}{2} Z_t \exp\left(-\frac{x}{\mu}\right) \cos\left(\frac{x}{\mu} + \omega t\right)$$

$$\lambda = 2\pi\mu \quad \text{Wave-length}$$

$$v_f = f\lambda = (\omega/2\pi)(2\pi\mu) = \mu\omega = (2\alpha\omega)^{1/2}$$

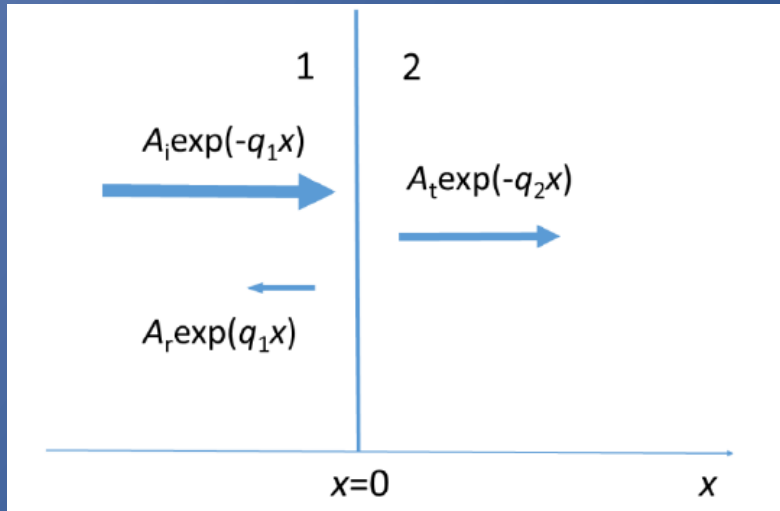
Phase velocity

$$v_g = 2v_f$$

Group velocity

THERMAL WAVES AND THEIR PROPERTIES

Behavior at interfaces (normal incidence)



$$T(x, t) = \begin{cases} A_i e^{-q_1 x} + A_r e^{q_1 x} & x < 0 \\ A_t e^{-q_2 x} & x > 0 \end{cases}$$

$$A_j = (I_0 / 2 \varepsilon \omega^{1/2}) \exp[i(\omega t - \pi/4)]$$

$$(j = i, r, t)$$

Temperature continuity at $x=0$
(negligible interfacial thermal resistance)

$$\rightarrow A_i + A_r = A_t$$

Heat flux continuity at $x=0$
(see Fourier's law)

$$\rightarrow A_i - A_r = (k_2 q_2 / k_1 q_1) A_t$$

$$A_t = 2 A_i / [1 + k_2 q_2 / k_1 q_1]$$

$$A_r = A_i [(1 - k_2 q_2 / k_1 q_1) / (1 + k_2 q_2 / k_1 q_1)]$$

Reflection and transmission coefficients

$$R_{12} = \frac{A_r}{A_i} = \frac{b_{12} - 1}{b_{12} + 1}$$

$$b_{12} = \frac{\varepsilon_1}{\varepsilon_2}$$

$$T_{12} = \frac{A_t}{A_i} = \frac{2 b_{12}}{1 + b_{12}}$$

THERMAL WAVES AND THEIR PROPERTIES

Depth profiling and imaging are possible !

$$\mu = \sqrt{\frac{2\alpha}{\omega}}$$

Orders of magnitude

$\lambda = 2\pi/k_w = 2\pi\mu$ Wave-length (k_w is the wave-number)

!TWs are fully damped within one wave-length!

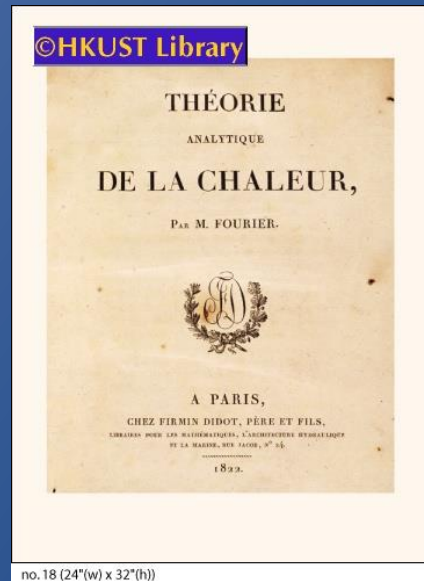
$v = \omega/k_w = \sqrt{2\alpha\omega}$ phase velocity

Typical solid material ($\alpha \approx 10^{-4} \text{ m}^2/\text{s}$)

For $f=10 \text{ kHz}$

$\mu \approx 10 \text{ }\mu\text{m}$ $\lambda \approx 30 \text{ }\mu\text{m}$ $v \approx 0.1 \text{ m/s}$

!The wave-length of acoustic waves at $f=1 \text{ kHz}$ is $\lambda_{\text{aw}} = v_{\text{aw}}/f \approx 1\text{cm}$, where $v_{\text{aw}} \approx 1000\text{m/s}$ is the sound velocity!



no.18 (24"(w) x 32"(h))

Jean Baptiste Joseph Fourier (1768-1830)

"The problem of the earth crust temperature is one of the most beautiful applications of the heat transfer theory"

J. B. J. Fourier

Home work: A very simple photothermal experiment

REVISTA MEXICANA DE FÍSICA E 52 (1) 21-27

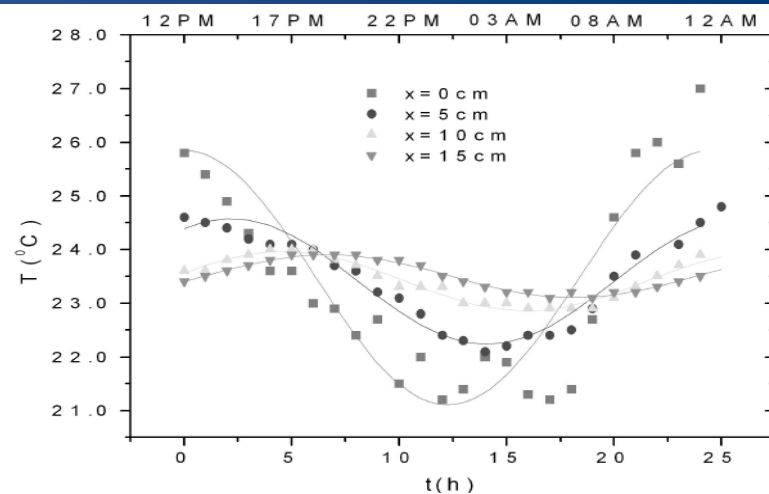


FIGURE 4. Soil Temperature as a function of time at different depths beneath the earth's surface and hourly air temperature. The solid curves represent best fits to Eq. (14) The air temperature ($x=0$) versus time curve is also represented for comparison.

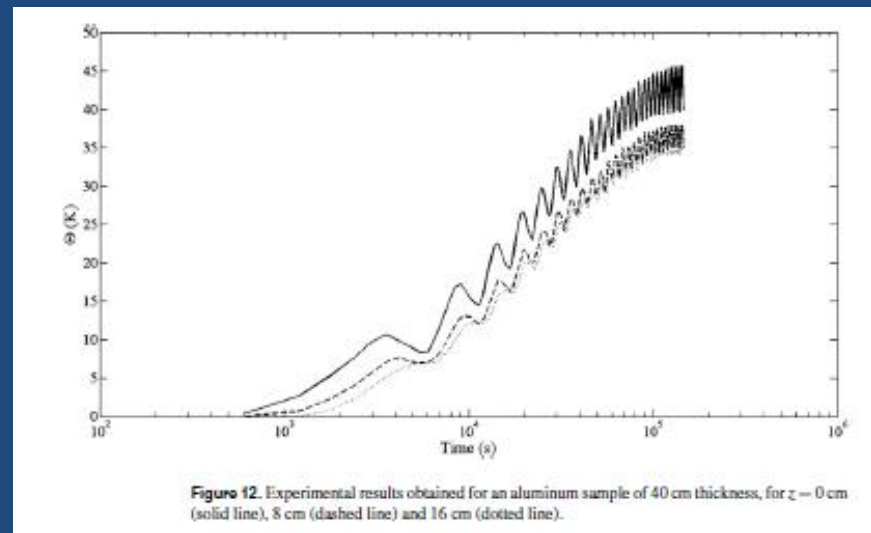
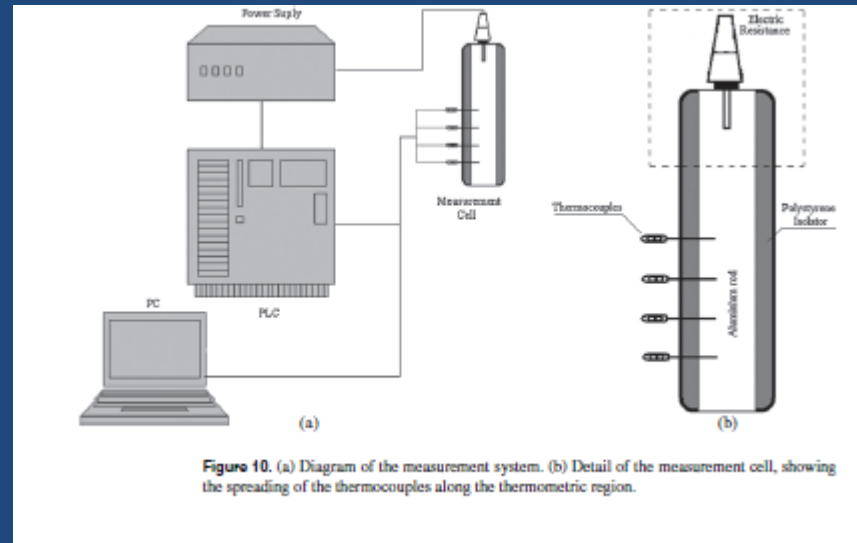
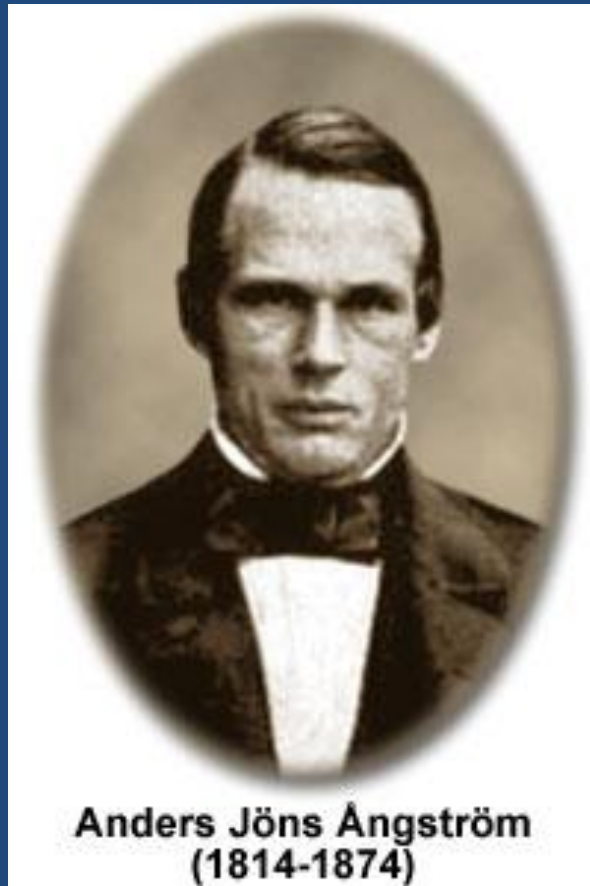
(1822's Théorie Analytique de la chaleur was first developed in 1807 under the name Théorie de la propagation de la Chaleur dans les Solides)



Adrien Marie Legendre (left) and **Joseph Fourier** (right)

Boilly, Julien-Leopold. (1820). *Album de 73 Portraits-Charge Aquarelle's des Membres de l'Institute* (water colour portrait #29).
Biliotheque de l'Institut de France.

Another 19th Century discovery: The Ångström method for thermal diffusivity measurement
 A. J. Ångström, *Ann. Phys. Chem.* 64:33 (1861)



THERMAL WAVES (with distributed heat source)

Isotropic and homogeneous semi-infinite solid + Bulk uniform light absorption (1D) + $\eta \neq 1$
+ $R \neq 0$ + neglecting heat losses

amount of heat generated per volume unit of the sample in an element of thickness dx at depth x

$$dQ = \eta(1-R)I_0\beta \exp(-\beta x) dx$$

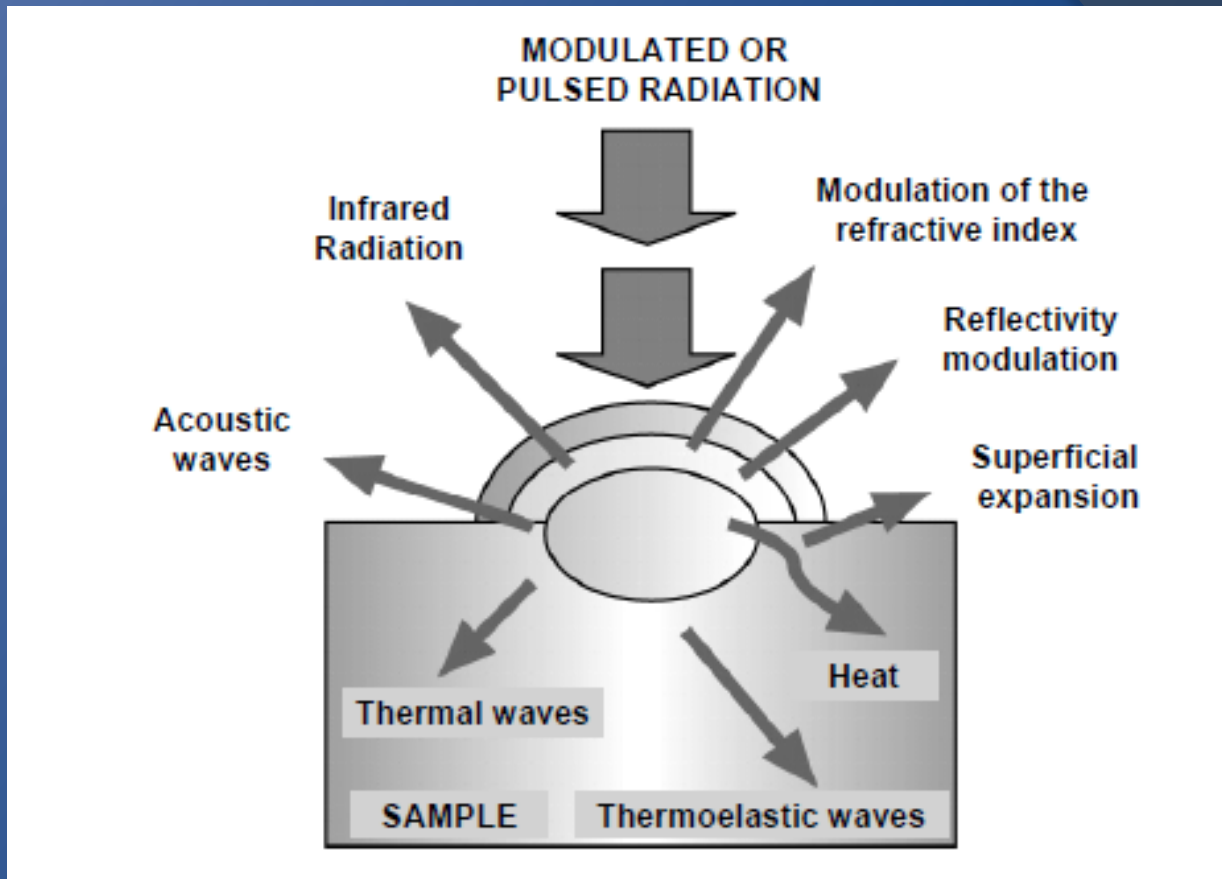
$$T(x, t) = \frac{I_0\eta(1-R)\beta}{2\varepsilon\sqrt{\omega}} \int_x^{x+dx} \exp(-\beta x') \exp(-qx') dx' \times \exp\left[-i\left(\omega t + \frac{\pi}{4}\right)\right]$$

$$T(x, t) = \frac{I_0\eta(1-R)}{2\varepsilon\sqrt{\omega}} \frac{\beta}{\beta+q} \exp[-(\beta+q)x] \exp\left[-i\left(\omega t + \frac{\pi}{4}\right)\right]$$

$\beta(\lambda) \rightarrow$ Spectroscopy is possible !

3RD PART: THE PHOTOTHERMAL TECHNIQUES

Besides using a microphone: How to detect?



PRINCIPLES OF PHOTOTHERMAL TECHNIQUES

Photothermal techniques available at Photothermal Techniques Laboratory, CICATA-Legaria



Thermal lens and photothermal modulated photoreflectance microscopy



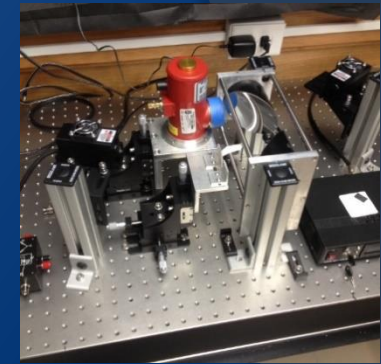
Thermal lens spectroscopy



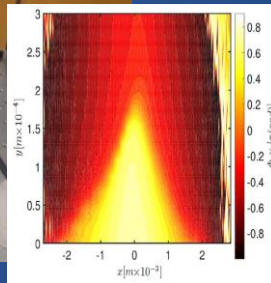
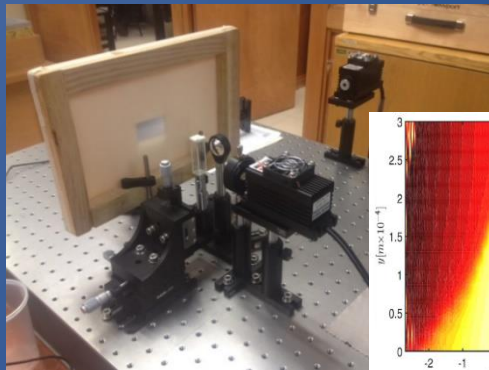
Photothermal Infrared thermography



Photoacoustic spectroscopy



Photothermal Infrared radiometry



Photothermal (multi) beam deflection and photothermal lock-in shadowgraphy

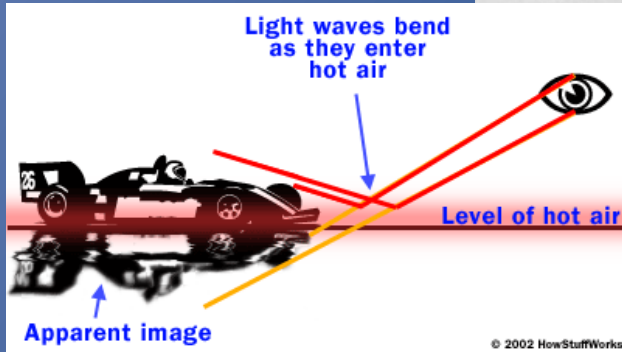


Photopyroelectric technique

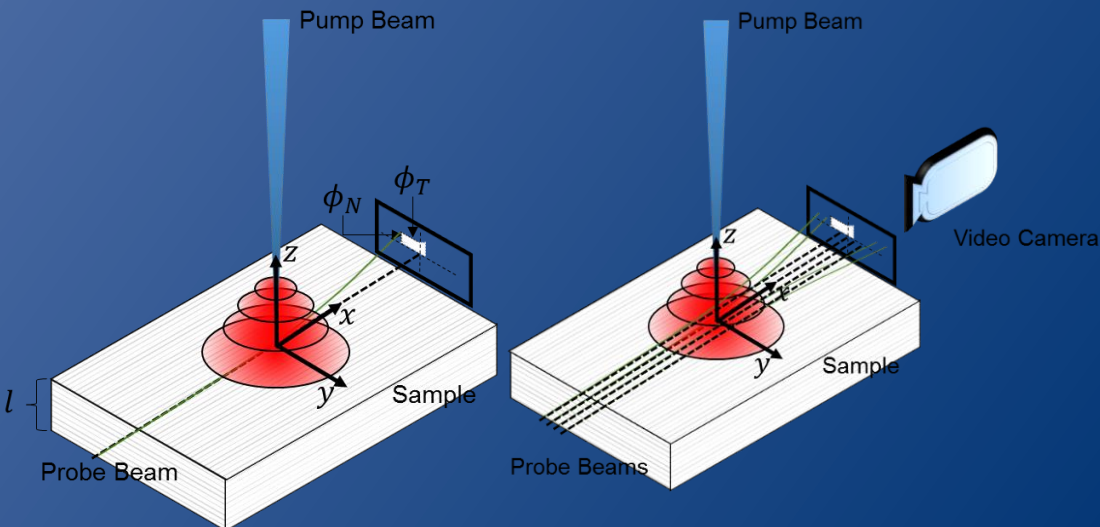


Photopyroelectric/acoustic microscopy

Another example of a photothermal technique:



Mirage effect (BEAM DEFLECTION)



Wednesday 9.00 h Photothermal digital lock-in shadowgraph technique for materials thermal characterization (signal and image digital processing) (Leonardo Building - Budinich Lecture Hall) !!

4TH PART: SELECTED APPLICATIONS

PA SPECTROSCOPY AND DEPTH PROFILING

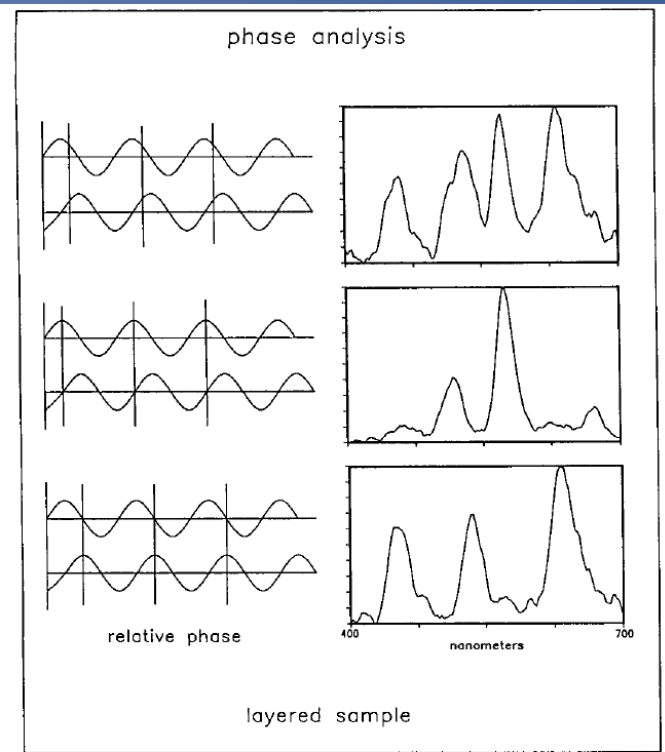


FIG. 6. An illustration of selective depth profiling using phase sensitive detection at a modulation frequency, f , of 13 Hz and corresponding thermal diffusion length of $37 \mu\text{m}$: (a) both layers contribute to the total photoacoustic signal; (b) maximization of the contribution from the surface layer; (c) maximization of the contribution from the interior layer.

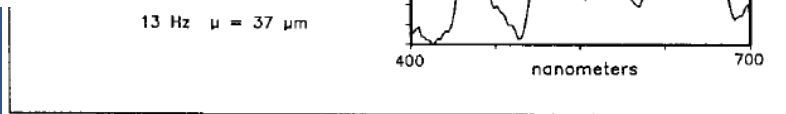


FIG. 4. An illustration of depth profiling by variation of the modulation frequency using the layered sample: (a) modulation frequency, f , 208 Hz; thermal diffusion length, μ , $9 \mu\text{m}$; (b) f , 26 Hz; μ , $26 \mu\text{m}$; (c) f , 13 Hz; μ , $37 \mu\text{m}$.

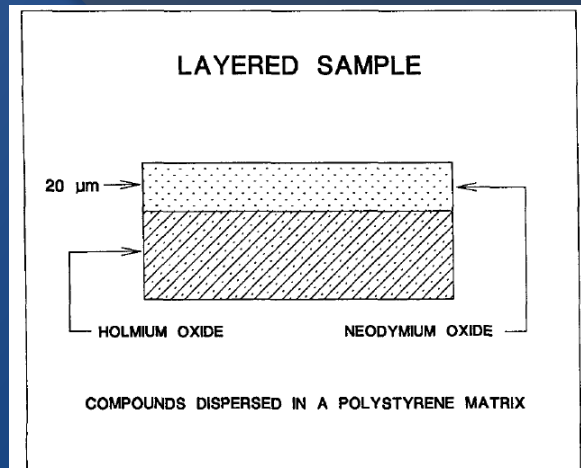


FIG. 2. Schematic diagram for the layered sample consisting of a thin ($20 \mu\text{m}$) surface layer of neodymium oxide on a thick (2.5mm) interior layer of holmium oxide.

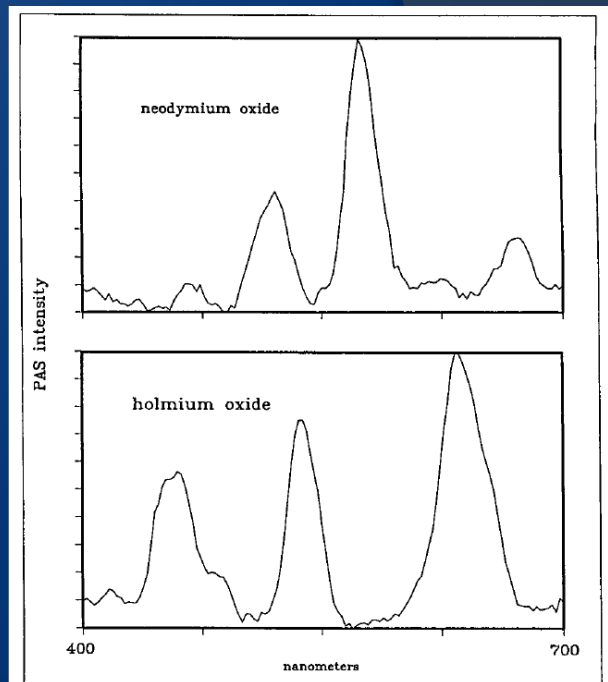


FIG. 5. Visible Hadamard transform photoacoustic spectra of neodymium oxide and holmium oxide.

More Spectroscopic Applications:

Thermal lens spectroscopy:

Prof. A. Marcano, Wednesday 15 and Thursday 16, 11.00 h

Thermal lens microscopy:

Prof. M. Franko Monday 20 and Tuesday 21, 11.00 h

+ some experimental sessions

THERMAL CHARACTERIZATION BY SLOPE METHOD

$$T(\mathbf{x}, t) = \frac{I_0}{2\varepsilon\sqrt{\omega}} \exp(-q\mathbf{x}) \exp\left[-i\left(\omega t + \frac{\pi}{4}\right)\right] = \frac{I_0}{2\varepsilon\sqrt{\omega}} \exp\left(-\frac{\mathbf{x}}{\mu}\right) \exp\left[-i\left(\frac{\mathbf{x}}{\mu} + \omega t + \frac{\pi}{4}\right)\right]$$

Amplitude

Phase

$$\mu = \sqrt{\frac{2\alpha}{\omega}}$$

$$\Delta\phi = \mathbf{x}/\mu + \pi/4$$

LOG (AMPLITUDE $\times \omega^{1/2}$) VERSUS $\omega^{1/2}$
 PHASE VERSUS $\omega^{1/2}$ } STRAIGHT LINE WITH SLOPE = $L/(2\alpha)^{1/2}$

FREQUENCY DEPENDENT INSTRUMENTAL FACTOR
 CAN AFFECT BOTH AMPLITUDE AND PHASE

→ NORMALIZATION PROCEDURES, EXPERIMENTAL ARTIFACTS, ETC

LOG (AMPLITUDE) VERSUS L
 PHASE VERSUS L } STRAIGHT LINE WITH SLOPE = $(\omega/2\alpha)^{1/2}$

STRAIGHTFORWARD PROCEDURES

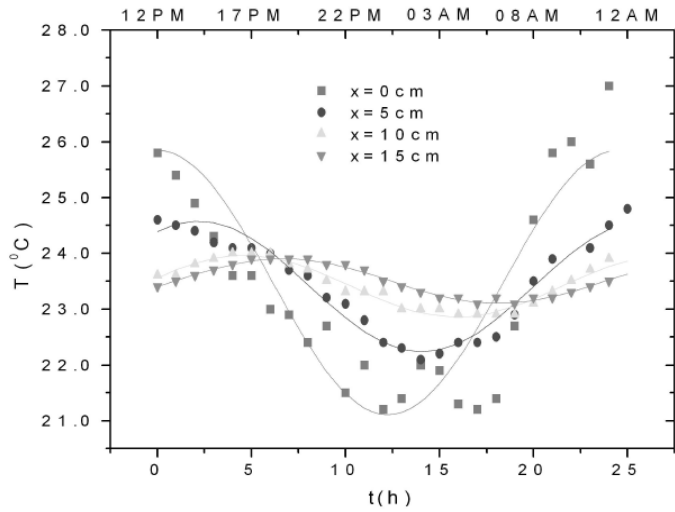


FIGURE 4. Soil Temperature as a function of time at different depths beneath the earth's surface and hourly air temperature. The solid curves represent best fits to Eq. (14) The air temperature ($x=0$) versus time curve is also represented for comparison.

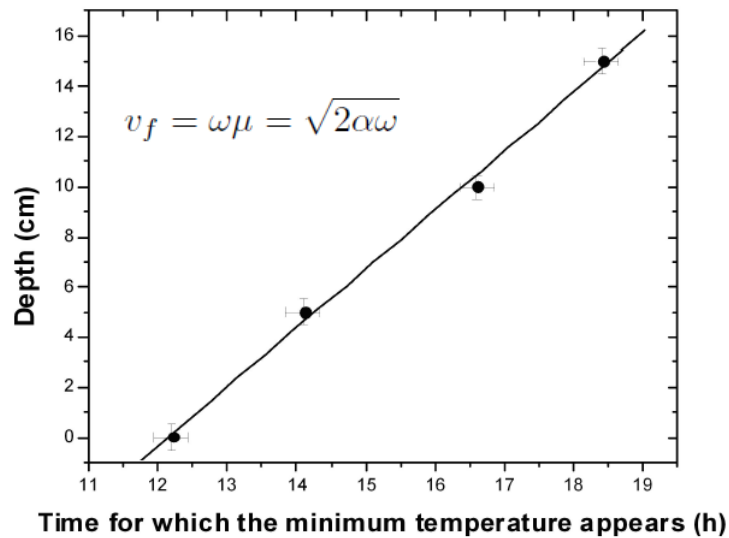


FIGURE 5. Depth at which the measurements were performed at a function of time at which the minimum temperature appears. The solid line is the best linear fit for the data.

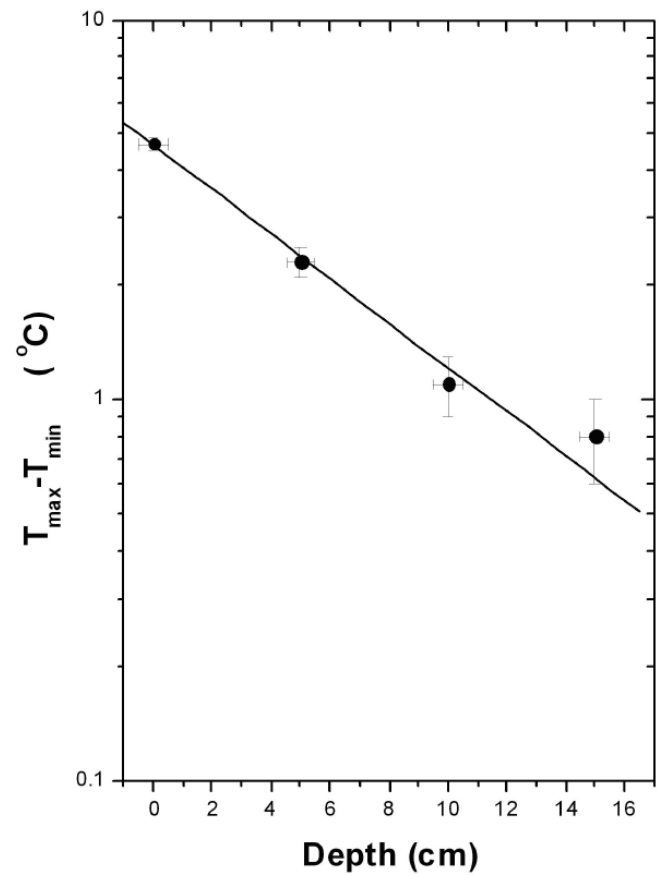


FIGURE 6. Logarithm of the thermal waves amplitudes as a function of depth. The solid line is the best linear fit for the data.

THE THERMAL WAVE RESONATOR CAVITY METHOD

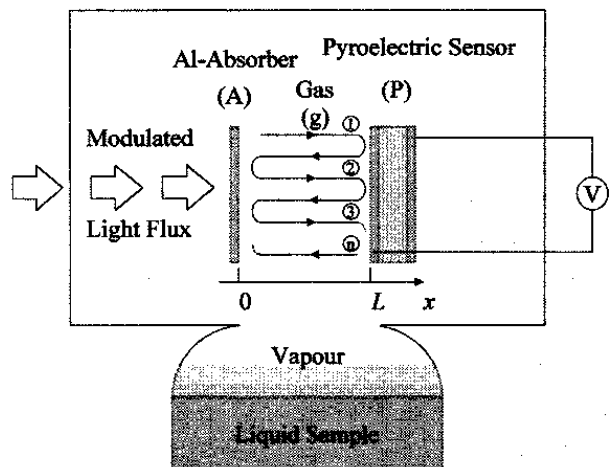


FIG. 1. Schematic view of the thermal wave resonator cavity sensor described in the text.

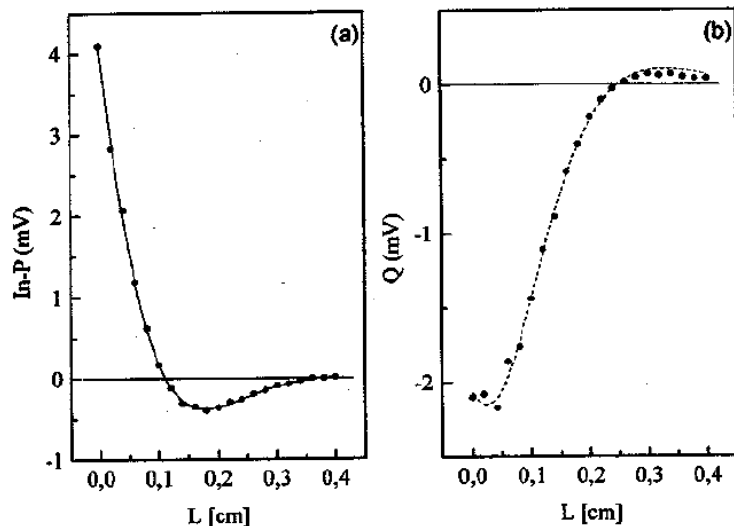


FIG. 2. In-phase (a) and quadrature (b) signals measured for air. The solid curves are the best-fit results to the real and imaginary parts of Eq. (6), respectively.

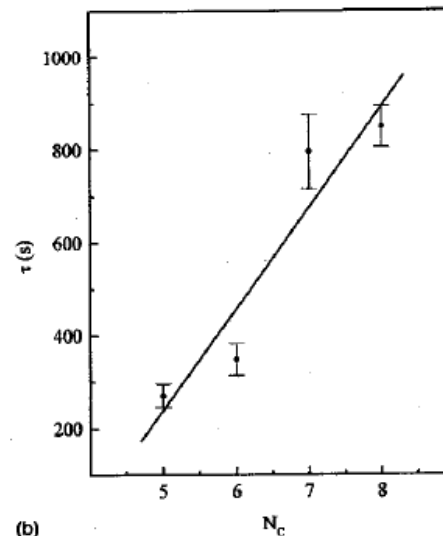
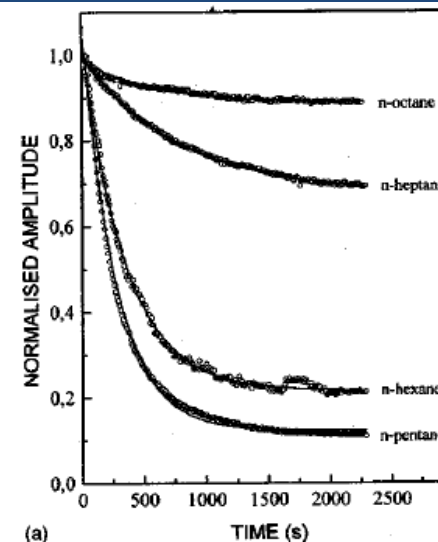


FIG. 3. (a) Time evolution (normalized signal as a function of time) of the TWRC signal corresponding to different hydrocarbon samples. The solid curves are the best-fit result of the data to an exponential decay law. (b) Decay time obtained from the fits represented in (a) as a function of the number of carbon atoms in the linear chain.

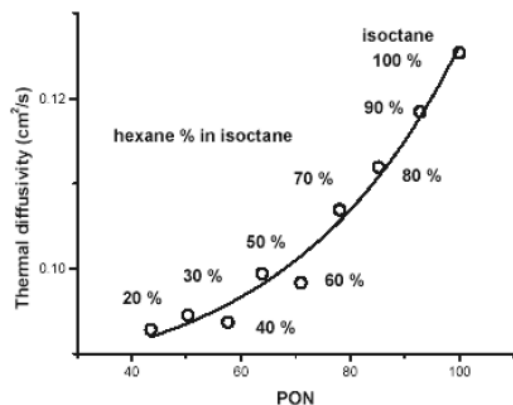


Figure 10. Thermal diffusivity versus Pump Octane Number for different concentrations of (liquid) *n*-hexane in isooctane. The solid curve is the best fit to an exponential growth function. (Taken from Ref. [76]).

Lima, J.A.P., Massunaga, M.S.O., Vargas, H. and Miranda, L.C.M. 2004, Anal. Chem. 76, 114.

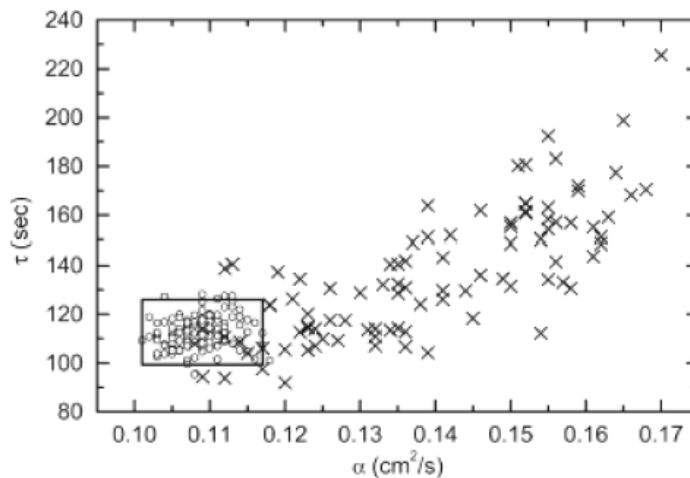


Figure 11. Correlation between the characteristic decay time and the thermal diffusivity for the 210 gasoline samples. The solid rectangle represents the conformity grid. Measurements were performed at 23°C, at $f=10$ Hz and $L=2$ mm (Reprinted in part with permission from Ref. [41]. Copyright 2004 American Chemical Society).

Thermal characterization of thin filaments



Spider silk ties scientists up in knots

Two years ago, researchers published a study which concluded that spider silk conducts heat as well as metals. Now scientists have repeated the experiment and the results throw this discovery into question.

<http://www.sciencedaily.com/releases/2014/01/140122091732.htm>

ADVANCED
MATERIALS
www.advmat.de

Materials
Views
www.MaterialsViews.com

New Secrets of Spider Silk: Exceptionally High Thermal Conductivity and Its Abnormal Change under Stretching

Xiaopeng Huang, Guoqing Liu, and Xinwei Wang*

Materials Letters 114 (2014) 1–3

Contents lists available at ScienceDirect

Materials Letters

ELSEVIER journal homepage: www.elsevier.com/locate/matlet

Revising the exceptionally high thermal diffusivity of spider silk

Raquel Fuente, Arantza Mendioroz, Agustín Salazar*

Departamento de Física Aplicada I, Escuela Técnica Superior de Ingeniería, Universidad del País Vasco UPV/EHU, Alameda Urquijo s/n, 48013 Bilbao, Spain

CrossMark

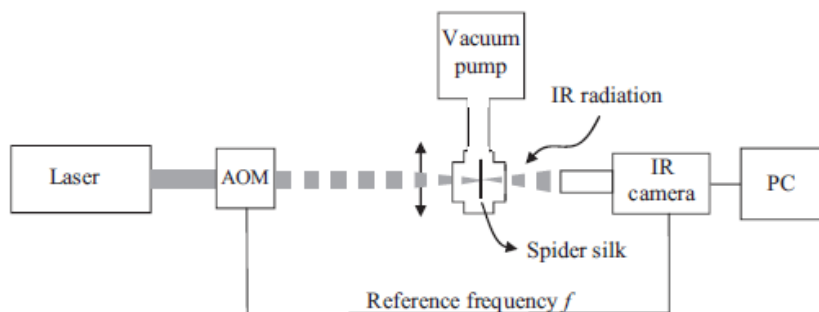


Fig. 1. Diagram of the experimental setup. The intensity of the laser is modulated by an acousto-optic modulator (AOM) and focused onto the spider silk filament. Then, IR radiation is emitted from the sample and detected by the IR camera, which processes the signal at the frequency reference (f) and sends the information to the PC for further analysis.

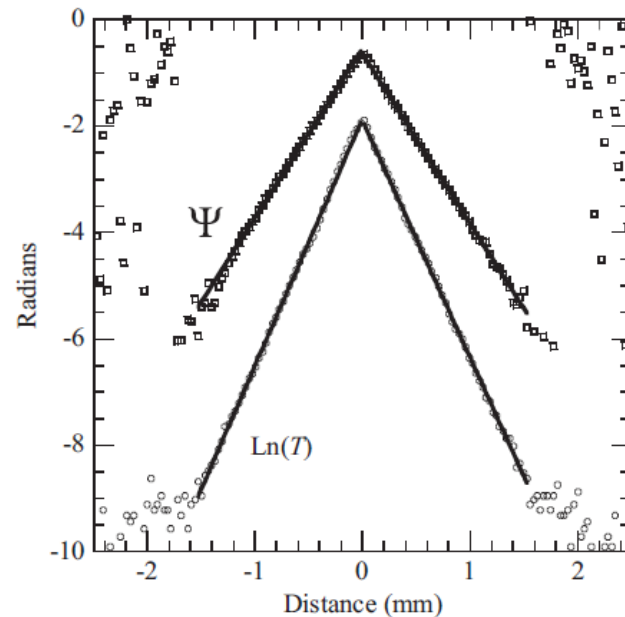
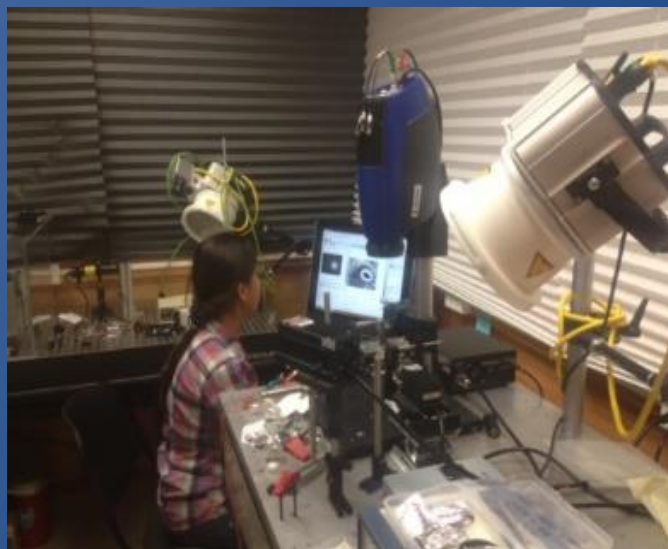


Fig. 2. Phase (ψ) and natural logarithm of the amplitude ($\ln(T)$) of a spider dragline temperature as a function of the distance to the heating spot, at $f=0.914$ Hz. Symbols correspond to experimental data and continuous lines to the linear fittings.



Thermal properties characterization:

Photothermal shadowgraph technique:

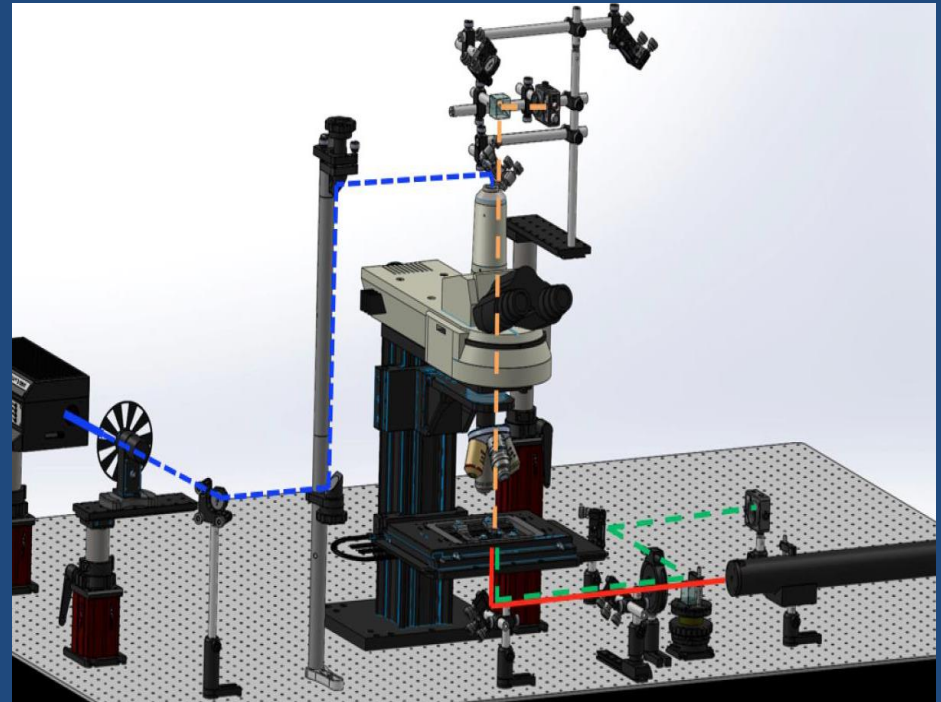
Prof. E. Marin, Wednesday 15, 9.00 h

+ SOME EXPERIMENTAL SESSIONS

Photothermal pump-probe optical methods are very useful for both spectroscopy and thermal characterization, e.g. thermal lens technique

$$\frac{\Delta\eta}{\eta_0} = \frac{1}{\eta_0} \frac{d\eta}{dT} \Delta T$$

Thermal lens spectroscopy (see Franko and Marcano forthcoming courses)

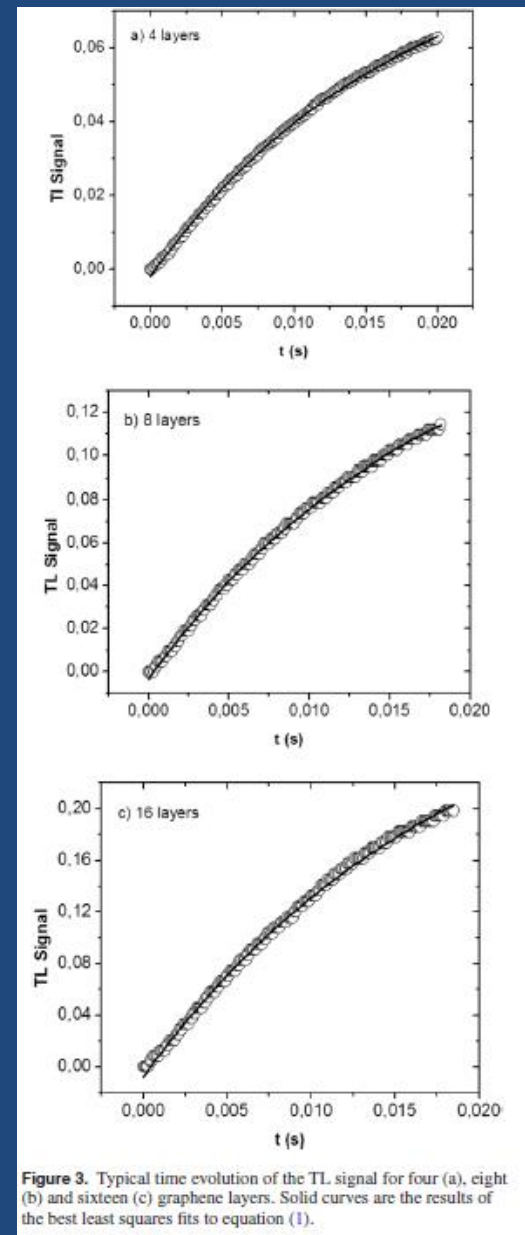
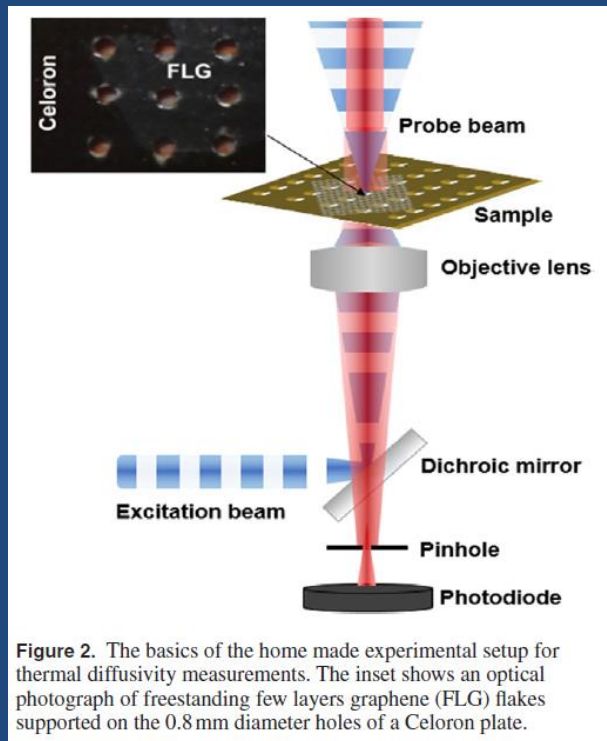
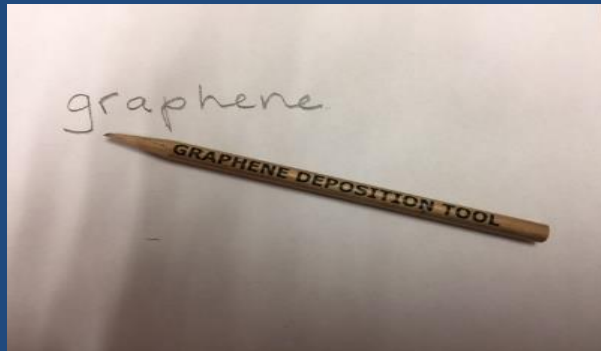


DOI:10.1364/BOE.6.003898 | BIOMEDICAL OPTICS EXPRESS 3898

J. Phys. D: Appl. Phys. 48 (2015) 465501

Laser Phys. Lett. 13 (2016) 055702

Graphene: 2D (semi) metal: a lattice of hexagonally arranged carbon atoms. The potential to produce graphene using a super abundant chemical element, and the possibility of its functionalization, make it a particular laboratory for basic research in 2D systems.



Signal ~ number of layers
→ imaging

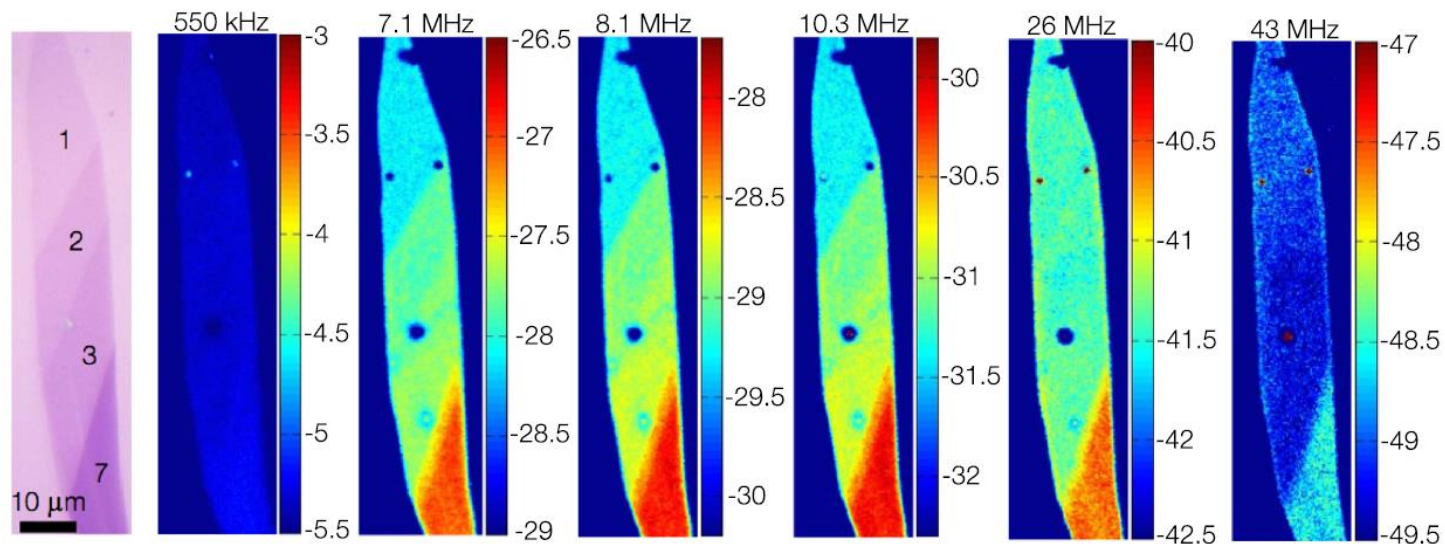


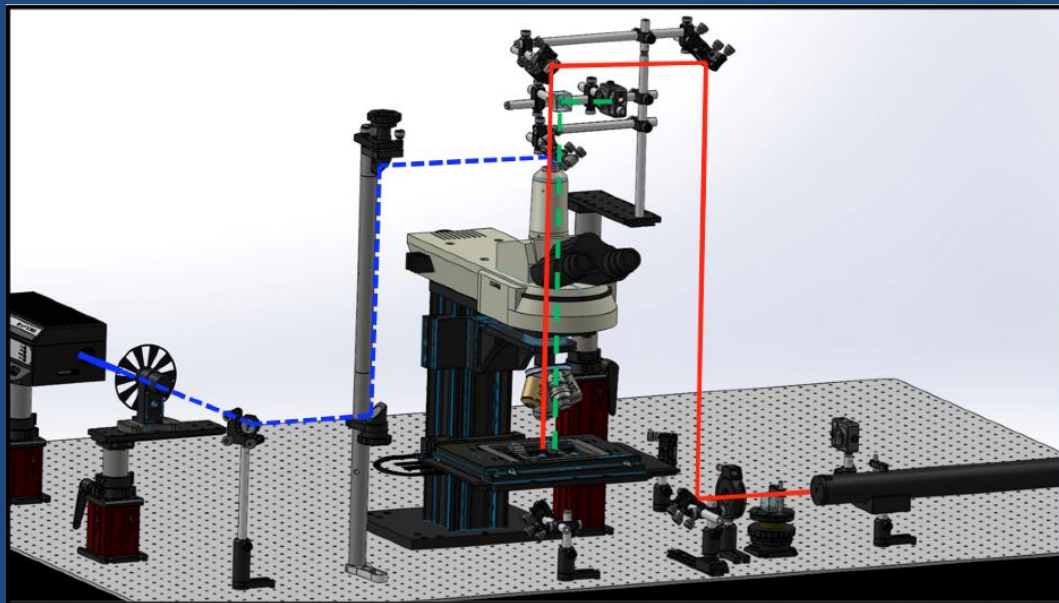
FIG. 6. Phase images of flake 1 acquired simultaneously at six frequencies: 550 kHz, 7.1 MHz, 8.1 MHz, 10.3 MHz, 26 MHz, and 43 MHz. The image contrast between the layers follows the sensitivity to G_{\parallel} shown in Fig. 5(e).

JOURNAL OF APPLIED PHYSICS **116**, 023515 (2014)

Images taken with a modulated thermoreflectance set-up

Modulated optical reflectance microscopy

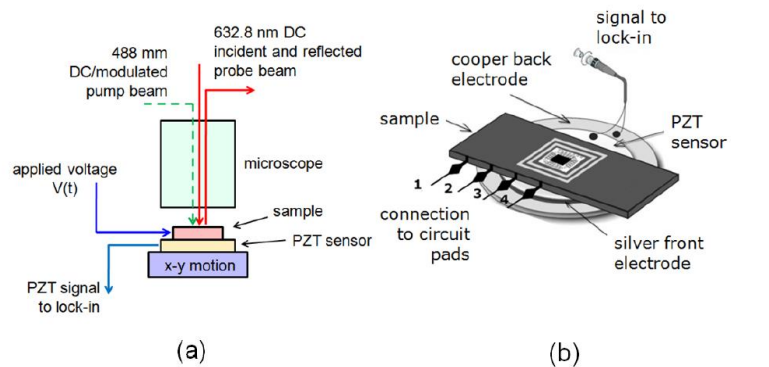
$$\frac{\Delta R}{R_0} = \frac{1}{R_0} \frac{dR}{dT} \Delta T$$



APPLIED PHYSICS LETTERS **109**, 041902 (2016)

Thermoacoustic and thermoreflectance imaging of biased integrated circuits: Voltage and temperature maps

APPLIED PHYSICS LETTERS **109**, 041902 (2016)



Figs. 3.1. (a) Block diagram of the experimental setup; (b) detailed view of the sample and PZT sensor.

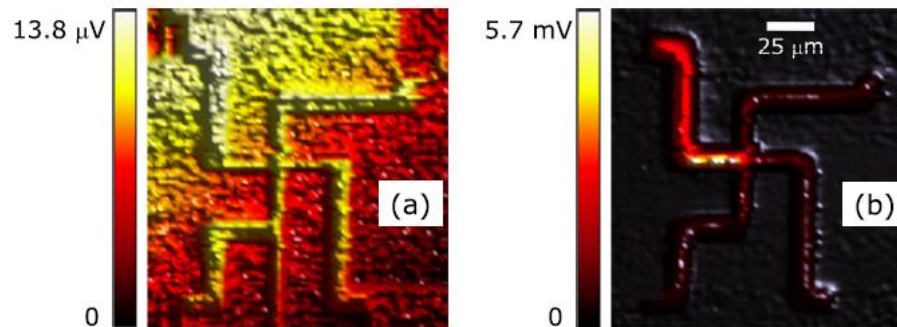
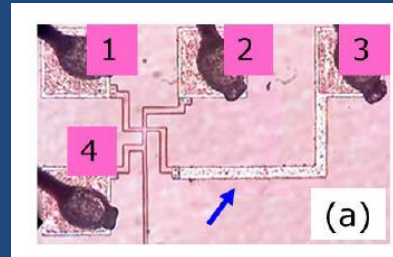


FIG. 3. (a) PZT and (b) thermoreflectance 2nd harmonic signal amplitude maps under modulated voltage excitation. Scanned area: $162 \mu\text{m} \times 173 \mu\text{m}$; modulated voltage: $V_0 = 4.0 \text{ V}$, $f = 25 \text{ kHz}$.

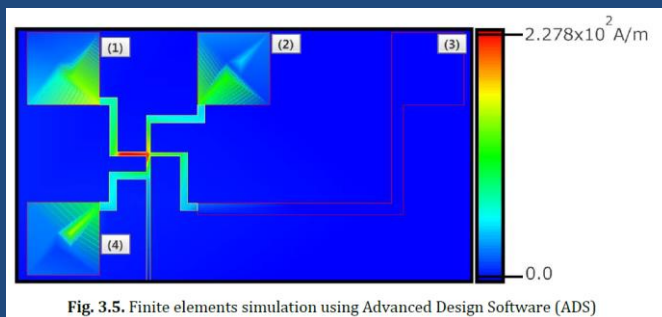
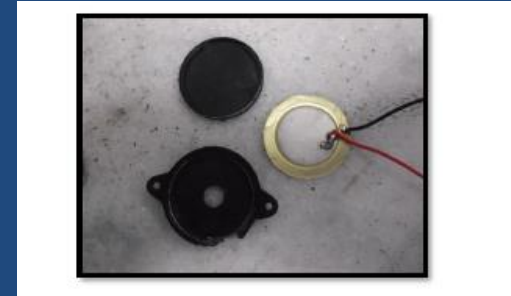
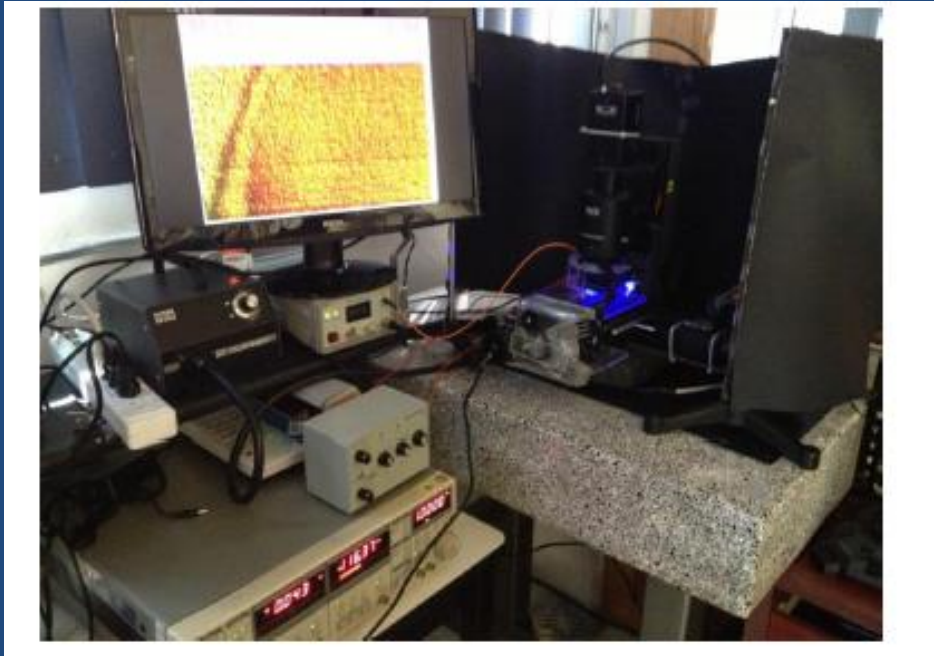


Fig. 3.5. Finite elements simulation using Advanced Design Software (ADS)

E. Hernández Rosales *et al* in preparation

Imaging

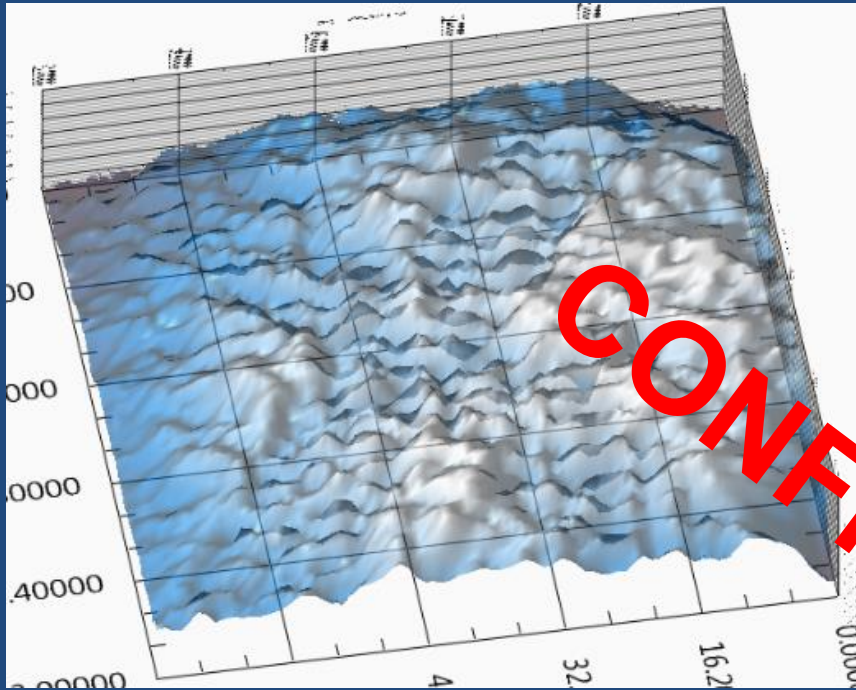
A photothermal microscope at CICATA-Legaria.



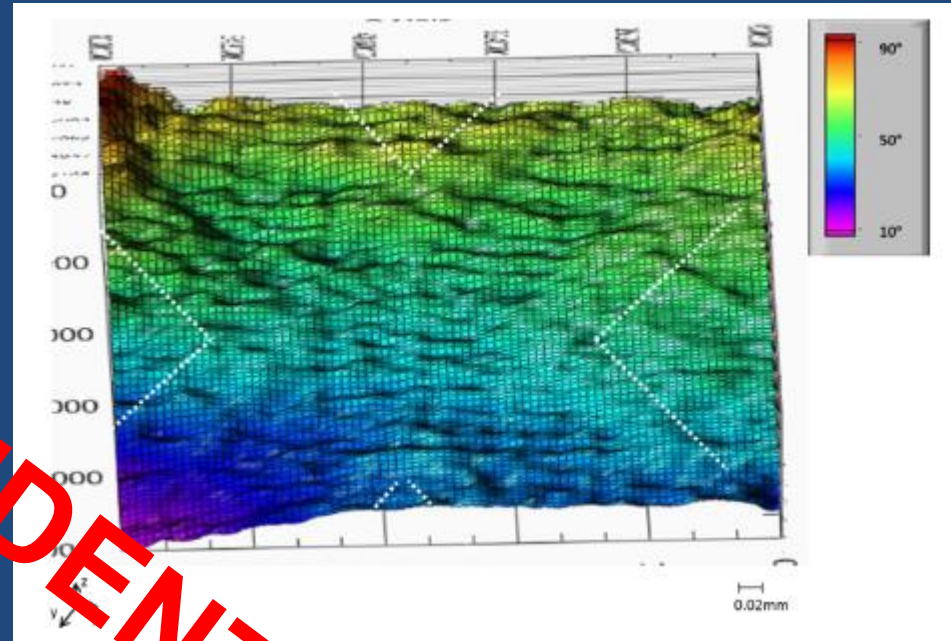
The sensor:
A PZT from a commercial buzzer

E. Cedeño, Master Thesis, CICATA-IPN, México, August 2013

Imaging



Amplitude image



Phase image

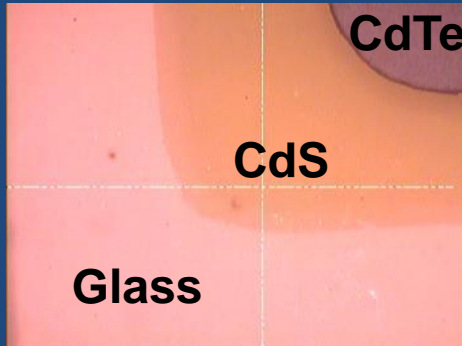


Optical image

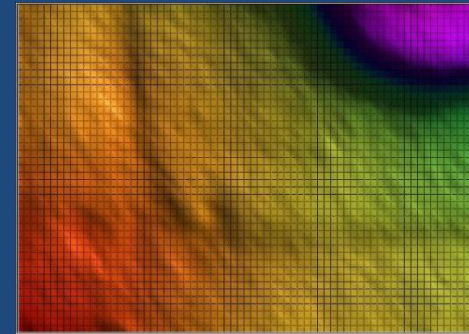
f=6 kHz
Resolution 0.02 mm
(7533 pixels)

Lottery Ticket "Raspe y Gane"

Imaging

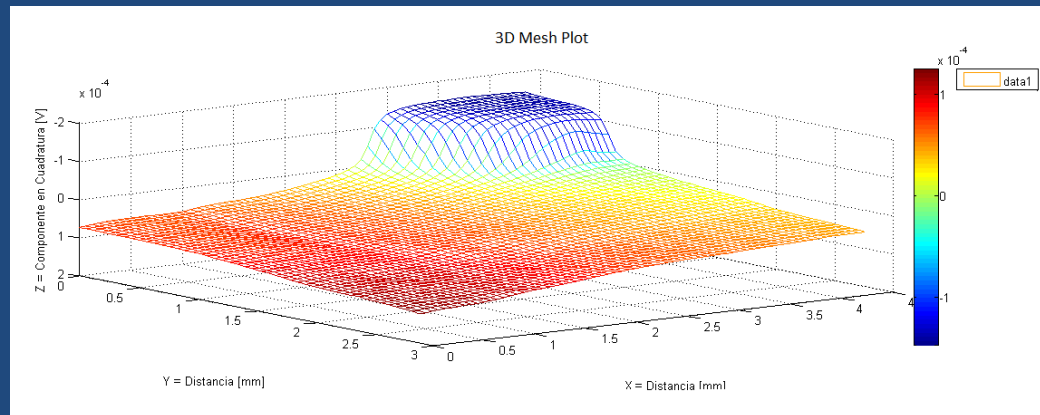
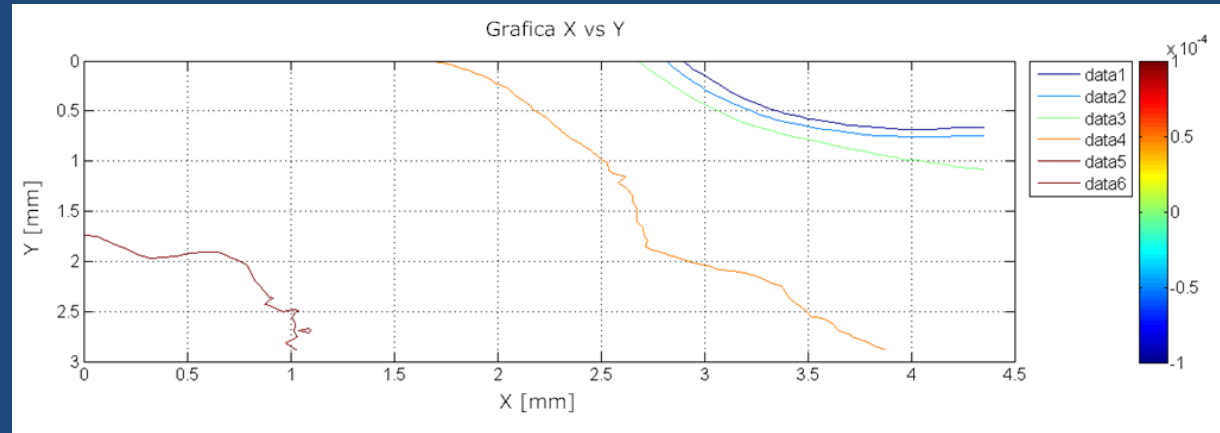


CdTe/CdS/Glass



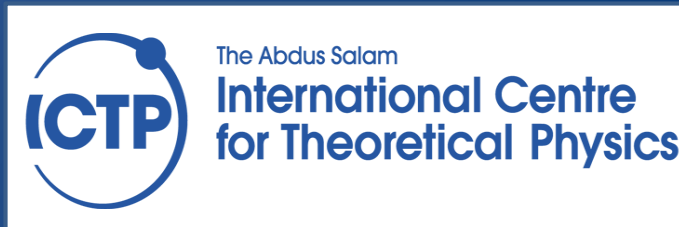
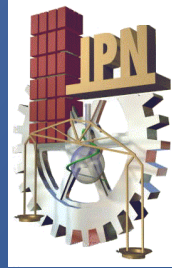
Optical

Photoacoustic



ACKNOWLEDGEMENTS

INSTITUTIONS:



COLLABORATORS:

MANY COLLEAGUES (IN MEXICO AND ABROAD) AND STUDENTS

Thank you!